Atmos. Chem. Phys. Discuss., 10, 26751–26812, 2010
www.atmos-chem-phys-discuss.net/10/26751/2010/
doi:10.5194/acpd-10-26751-2010

Atmospheric Chemistry and Physics Discussions

Reconstructing ozone chemistry from Asian wild fires using models, satellite and aircraft measurements during the ARCTAS campaign

R. Dupont[1], B. Pierce[2], J. Worden[1], J. Hair[3], M. Fenn[4], P. Hamer[1], M. Natarajan[3], T. Schaack[5], A. Lenzen[5], E. Apel[6], J. Dibb[7], G. Diskin[3], G. Huey[8], A. Weinheimer[6], and D. Knapp[6]

[1]Jet Propulsion Laboratory, California Institute of Technology, Pasadena, CA, USA
[2]NOAA/NESDIS/STAR, Madison, WI, USA
[3]NASA Langley Research Center, Hampton, VA, USA
[4]Science Systems and Applications, Inc, Hampton, VA, USA
[5]Space Science and Engineering Center, University of Wisconsin, Madison, WI, USA
[6]National Center for Atmospheric Research, Boulder, CO, USA
[7]University of New Hampshire – EOS, Durham, NH, USA

[8]School of Earth and Atmospheric Sciences, Georgia Institute of Technology, Atlanta, GA, USA

Received: 22 September 2010 – Accepted: 5 October 2010 – Published: 8 November 2010

Correspondence to: R. Dupont (richard.dupont@jpl.nasa.gov)

Published by Copernicus Publications on behalf of the European Geosciences Union.

Abstract

We use ozone (O_3) and carbon monoxide (CO) satellite measurements from the Tropospheric Emission Spectrometer (TES), simulations from the Real-time Air Quality Modeling System (RAQMS) and aircraft data from the NASA DC8 aircraft to characterize the chemical and dynamical evolution of Asian wildfire plumes during the spring ARCTAS campaign 2008. On the 19 April, NASA DC8 O_3 and aerosol Differential Absorption Lidar (DIAL) observed two biomass burning plumes originating from North-Western Asia (Kazakhstan) and South-Eastern Asia (Thailand) that advected eastward over the Pacific reaching North America in 10 to 12 days. Using both TES observations and RAQMS chemical analyses, we track the wildfire plumes from their source to the ARCTAS DC8 platform. Comparison between satellite O_3 and CO measurements and model results show consistency when the TES averaging kernel and constraint vector are applied to the model. However, RAQMS CO simulations suggest that TES observations do not capture the full range of CO variability in the plume due to low sensitivity. In both plumes, exchanges between the stratosphere and the troposphere tend to be a major factor influencing O_3 concentrations. However, fire emissions of ozone precursors increase photochemical ozone production, particularly in the Thailand wildfire plume. Analysis shows that the Kazakhstan plume is responsible for increases of O_3 and CO mixing ratios up to 6.4 ppbv and 38 ppbv in the lower troposphere, and the Thailand plume is responsible for increases of O_3 and CO mixing ratios up to 11 ppbv and 71 ppbv in the upper troposphere.

1 Introduction

Wildfire emissions affect atmospheric composition on global scales (Andreae, 1983; Reichle et al., 1986; Fishman et al., 1990; Soja et al., 2007) with levels of carbon monoxide (CO), carbon dioxide (CO_2) and nitrogen oxides (NO_x) comparable to fossil fuel emissions (Seiler and Crutzen, 1980; Crutzen and Andreae, 1990). During

the last decade, measurement from satellites, aircraft, and ground-based observations have confirmed significant concentrations of CO, O_3 and other trace gases in regions affected by biomass burning (Thompson et al., 1992). Van der Werf et al. (2006) showed that global emissions of CO from biomass burning were 15% larger than fossil fuel emissions (750 $Tg\,y^{-1}$). Similarly, global biomass burning emissions of N_2O, CO_2, NO_x could respectively represent 70% (1.4 $Tg\,y^{-1}$), 60% (14 300 $Tg\,y^{-1}$) and 50% (22.5 $Tg\,y^{-1}$) of global fossil fuel emissions.

Satellite data have allowed monitoring of the large numbers of seasonal fires over Siberia/northeast Asia (Cahoon et al., 1994; Tanimoto et al., 2000; Kajii et al., 2002; Kato et al., 2002; Soja et al., 2004) and over the Southeast Asian subcontinent (Christopher et al., 1998; Goloub and Arino, 2000). Consequently, Asian fires can represent 10% of global Carbon emissions (Van der Werf et al., 2006). Those fires play an important role in total tropospheric CO concentrations and interannual variability in the Northern Hemisphere (Novelli et al., 2003; Edwards et al., 2004; Kasischke et al., 2005; Pfister et al., 2005; Nedelec et al., 2005; Fisher et al., 2010).

Aircraft and ground-based measurements have shown that Asian fires can influence O_3 concentrations over North America (Jaffe et al., 2004; Morris et al., 2006), the Arctic (Warnecke et al., 2008) and even Europe (Simmonds et al., 2005). For example, Bertschi and Jaffe (2005) have shown that Siberian fires have caused three ozone pollution events over the coast of Washington state in 2002. However, the impact of fires on tropospheric O_3concentrations is challenging to estimate. Indeed, O_3 production is highly variable inside boreal fire plumes because of the influence of clouds and aerosols on photochemical production as well as highly variable PAN and NO_x concentrations and the cycling between these species (Mauzerall et al., 1996; Lapina et al., 2006; Val Martin et al., 2006; Real et al., 2007; Verma et al., 2009).

During spring 2008, fires burned throughout Asia and Siberia. Smoke from these fires was observed across the Pacific by satellite and aircraft measurements during the ARCTAS/ARCPAC campaign. In this paper we use fire counts from the MODIS satellite instrument, CO and O_3 profiles from Tropospheric Emission Spectrometer (TES), in

situ measurements from ARCTAS aircraft data and the Real-time Air Quality Modeling System (RAQMS) to understand the factors influencing O_3 production and transport from these Asian fires and their impact on middle and high latitude tropospheric chemistry.

2 Overview of ARCTAS campaign

2.1 Spring ARCTAS 2008

The NASA ARCTAS field campaign consisted of two phases; a spring and summer deployment and was part of the international IPY/POLARCAT arctic field program for atmospheric composition (http://zardoz.nilu.no/~andreas/POLARCAT/), which involved a consortium of countries (e.g., United States, Canada, Germany, France, Norway, Russia...) several aircraft, surface, and shipbased measurement platforms.

The Spring phase of the ARCTAS campaign took place as 3-week aircraft deployments in April 2008. It involved the NASA DC8 as an airborne platform for detailed atmospheric composition and two smaller aircraft to focus more closely on aerosols and radiation. As a complement to aircraft measurement NASA's polarorbiting satellites (Terra and the Atrain) observe the longrange transport of pollution and its seasonal accumulation in the Arctic, enabling a better understanding of pollution sources, transport pathways, and radiative impacts of boreal smoke plumes.

ARCTAS has four major scientific themes, including the impact of Boreal forest fires on atmospheric composition, and long-range transport of pollution to the Arctic including tropospheric ozone. As an atmospheric receptor of long-range transport of pollutants from the northern midlatitudes continents (Shaw, 1995; Quinn et al., 2007), the Arctic is increasingly beset by emissions from massive forest fires in boreal Eurasia (Hao and Ward, 1993; Cahoon et al., 1994; Tanimoto at al., 2000; Fromm et al., 2000; Dlugokenchy et al., 2001; Conard et al., 2002; Kasischke and Bruhwiler, 2003). However, there remain large uncertainties regarding the transport pathways and the relative

contributions of different source regions to arctic pollution (Staudt et al., 2001; Heald et al., 2003a; Liu et al., 2003; Liang et al., 2004; Koch and Hansen, 2005; Stohl, 2006; Shindell et al., 2008; Turquety et al., 2008; Shindell et al., 2008; Yashiro et al., 2009; Fisher et al., 2010; Jacob et al., 2010). Integration of satellite and aircraft observations with models through ARCTAS provides a means to address this issue (Eckhardt et al., 2003; Klonecki et al., 2003; Koch and Hansen, 2005; Stohl, 2006; Shindell et al., 2008). Spacebased observations of CO and ozone from the Tropospheric Emission Spectrometer (TES) are of particular interest for characterizing synoptic transport events, the seasonal buildup of pollution during winter and spring and ventilation of the Arctic to midlatitudes in spring and summer.

Another major focus of ARCTAS is to evaluate chemical transport model (CTM) simulations of sourcereceptor relationships for pollutants in the Arctic which is a challenge because of the complexity of the transport patterns involved, the paucity of meteorological data, the stratification of the atmosphere, and uncertain chemistry and surface interactions.

2.2 Overview of DC8 aircraft in situ data during flight 11 (19 April 2008)

During April 2008, MODIS fire count (Fig. 1) shows large and relatively intense wildfires taking place in Asia, particularly in Kazakhstan, Siberia and Thailand. This agrees with previous observations by the Advanced Very High Resolution Radiometer (AVHRR) over Siberia and North Asia (Cahoon et al., 1994; Tanimoto et al., 2000; Kajii et al., 2002; Kato et al., 2002) and Southeast Asia (Christopher et al., 1998; Goloub and Arino, 2000). On the 19 April, during flight 11 between Fairbanks (Alaska) and Palmdale (California), the DC8 aircraft sampled several biomass-burning plumes, as identified based on in situ measurements (Fig. 2). The DC8 took off around 19:00 GMT (11:00 ADT) and landed approximately at 24:51 UTC (05:51 p.m. PDT) and remained along the OMI/TES track until around 22:51 UTC. The aircraft flew between 2 and 9 km to sample several biomass burning plumes. Using the DIfferential Absorption Lidar (DIAL) measurements, the altitude and thickness of the plumes were detected and

allowed vertical profiling through them measuring chemical and aerosol composition with the in situ sensors aboard the aircraft.

2.2.1 DIfferential Absorption Lidar (DIAL)

During DC8 flight 11, the DIfferential Absorption Lidar (DIAL) instrument measured elevated concentrations of O_3 and aerosols in what appeared to be two biomass burning plumes (Figs. 3 and 4). Figure 3 shows Aerosol Scattering Ratio (ASR) profiles measured by DIAL during DC8 flight 11 as a function of UTC time, latitude and longitude. The ASR is defined as the ratio of the attenuated aerosol backscatter laser light to the calculated molecular backscatter expected from an aerosol free atmosphere (Browell, 2001).

Values of ASR (591 nm) ranging from 0.1 to 5.0 and showing high concentrations of aerosols were observed in the lower and middle troposphere (2 to 6 km) all along the flight track. Forward model trajectories from the wildfire locations (Sect. 3.1) indicate that this plume originated primarily from the Kazakhstan and Baikal fires with contributions from anthropogenic emissions. In the same way, aerosols were detected in the upper troposphere (8 to 12 km) between 45 and 55° of latitude North. Forward model trajectories from the wildfire locations (Sect. 3.1) indicate that this plume came from the Thailand fires. Both middle and upper tropospheric plumes showed enhanced ozone concentrations relative to the background as seen in Fig. 4. In the same figure, O_3 concentrations higher than 125 ppbv are observed in the upper troposphere around 56° of latitude north (20:00 UTC time). This is the result of a stratospheric air mass descent and is not due to wildfires.

2.2.2 In situ measurements of plume chemical composition

The NASA DC8 aircraft flew through two parts of the lower-middle tropospheric fire plume between 55° N and 50° N (20:00 to 21:00 UTC) and around 40° N (around 23:00 UTC). In situ measurements showed high levels of Carbon monoxide (CO),

methanol (CH_3OH), acetone ($(CH_3)_2OH$), Black Carbon (BC) and Scattering Aerosol (SA) as well as PeroxyAcyl Nitrate (PAN) concentrations as elevated as expected in fire plumes (Figs. 5 and 6). Significant Sulfur dioxide (SO_2) concentrations, up to 450 pptv, were also measured in both parts of the fire plume suggesting anthropogenic influences possibly resulting from mixing of anthropogenic pollution with the boreal smoke plumes. In situ measurements showed O_3 concentrations of as high as 140 ppbv (Fig. 6). Unfortunately, no in situ sampling of the high tropospheric plume was performed.

Figure 5 shows CO (blue dots), SO_2 (green dots) and BC (red dots) concentrations along the DC8 flight track as a function of UTC time. Lower/middle tropospheric biomass burning plume, originated from Kazakhstan, was sampled in two sections between 20:00 and 21:10 UTC, and around 23:00 UTC. Both parts show high CO, SO_2 and BC levels respectively up to 400 ppbv, 125 pptv and 250 particles per cm^3 in the northern part (55° N, 20:00–21:10 UTC) and 220 ppbv, 450 pptv and 220 particles per cm^3 in southern part (40° N, 23:00 UTC). Those high levels of CO (Roths and Harris, 1996; Jaffe et al., 1997; Yurganov et al., 1998; Ponchanart et al., 2003; Fisher et al., 2010) and aerosols (Haywood and Boucher, 2000; Zhao et al., 2002; Eck et al., 2003; Myhre et al., 2003; Massie et al., 2004; Abel et al., 2005; Reid et al., 2005a, b; Forster et al., 2007) observed by in situ data point to the biomass burning origin of the plumes. Moreover, SO_2 measurements are significantly above background levels in both part of the lower/middle tropospheric plume; these enhanced amounts suggest mixing of the biomass burning plume with anthropogenic pollution.

Figure 6 shows higher concentrations of PAN (up to 2500 pptv) (blue dots) in the northern part of the plume. PAN is an important source and sink of NO_x with higher temperatures leading to NO_x production from PAN and lower temperatures leading to PAN production from NO_x. PAN can be produced from NO_x present in biomass burning plumes (Mauzerall et al., 1998; Real et al., 2007). Then, concentrations of NO_x and PAN will depend on plume temperature (Singh and Hanst, 1981). The plume has been transported in the middle troposphere and at high latitude (50–55° N) where

temperatures are low and PAN is stable leading to high PAN concentrations. Figure 6 shows O_3 (green dots) and NO_x (red dots) concentrations along the flight track as a function of UTC time. Both parts of the plume show high concentrations of NO_x (90–100 pptv in average) and also high level of O_3 with mean concentration of 90 ppbv that is 30 to 40 ppbv above background level.

In summary, the aircraft data suggest that the observed plumes in the middle and lower troposphere could originate from biomass burning and were subsequently mixed with anthropogenic pollution. We use these aircraft data along with forward wildfire trajectories and CO and ozone profile measurements from TES as well as the RAQMS model to confirm the biomass burning origin of these plumes and explain the ozone distributions observed during NASA/DC8 flight 11 on the 19 April 2008. We identify plume sources and reconstruct the chemical evolution of these plumes in Sect. 3 using the TES satellite data and RAQMS model and estimate the contribution to ozone from photochemistry and exchange from the stratosphere.

2.3 Overview of TES

TES is an infrared Fourier transform spectrometer that measures the thermal emission of the Earth's surface and atmosphere over the spectral range 650–2250 cm^{-1}. It was designed to provide simultaneous vertical profile retrievals of tropospheric O_3, CO and other trace gases on a global basis (Beer et al., 2001; Beer, 2006). The nadir footprint is 5.3 km across the spacecraft ground track and 8.5 km along track for the 16-detector average (Beer et al., 2001). TES has two basic science operating modes: Global Survey and Special Observations. Global Surveys are conducted every other day while special observations are taken as needed in between Global Surveys. We used global survey observations of TES O_3 and CO obtained between 7 April and 19 April 2008 with a nadir sampling of 1.6° spacing along the ground track.

The analysis presented here utilizes TES version 003 data (Osterman et al., 2007). An overview of the TES retrieval algorithm and error estimation are discussed by Bowman et al. (2006) and the characterization of errors and vertical information for

individual TES profiles are discussed by Worden et al. (2004) and Kulawik et al. (2006). The vertical resolution of TES nadir O_3 retrievals is about 6 km for cloud-free scenes, with sensitivity to both the lower and upper troposphere (Worden et al., 2004; Bowman et al., 2006). To date, TES tropospheric O_3 validation has been conducted through comparisons with ozonesondes (Worden et al., 2007) and lidar (Richards et al., 2008). These validation studies show that TES O_3 estimates are typically biased high in the upper troposphere by approximately 10%. Nassar et al. (2008) shows that TES O_3 is biased high by 3–10 ppb in the upper troposphere.

2.4 Real-time Air Quality Modeling System: overview

Chemical and aerosol analyses from the Real-Time Air Quality Modeling System (RAQMS) and ensemble wild fire trajectories are used to examine the different processes influencing the evolution of trace gases (e.g., O_3 and CO) within fire plumes prior to sampling these plumes by the DC8. RAQMS is a unified (stratosphere/troposphere), online (meteorological, chemical, and aerosol) modeling system which has been developed for assimilating satellite observations of atmospheric chemical composition and providing real-time predictions of trace gas and aerosol distributions (Pierce et al., 2003, 2007; Kittaka et al., 2004). The chemical formulation follows a family approach with partitioning on the basis of photochemical equilibrium approximations. The non-methane hydrocarbon (NMHC) chemical scheme is based on the carbon bond lumped structure approach (Pierce et al., 2007). Photolytic rates are calculated using the FAST-JX code, an updated version of FAST-J2 code (Bian et al., 2003). The RAQMS aerosol model incorporates online aerosol modules from GOCART (Chin et al., 2002, 2003). Seven aerosol species (SO_4, hydrophobic and hydrophilic organic carbon (OC), and black carbon (BC), dust, sea-salt) are transported. RAQMS biomass burning emissions use twice daily ecosystem/severity based emission estimates coupled with Moderate-Resolution Imaging Spectroradiometer (MODIS) Rapid Response fire detections (Al-Saadi et al., 2008). Total direct carbon emissions are calculated as the product of area burned and the ecosystem- and severity-specific

carbon consumption estimates. Ecosystem-dependent carbon consumption databases for three classes of fire severity (low, medium, and high) are considered. Fire weather severity is estimated using the US Forest Service Haines Index, which considers atmospheric moisture and thermal stability (Haines, 1988). Emissions of other species are determined by combining published emission ratios for different ecosystems (Cofer et al., 1991; Andreae and Merlet, 2001).

The RAQMS chemical analysis used in the current study is from a retrospective 4-month (February–May 2008) $2 \times 2^{\circ}$ assimilation that includes assimilation of cloud cleared OMI total column O_3 measurements and stratospheric O_3 profiles from the Microwave Limb Sounder (MLS) on the NASA Aura satellite. MODIS Aerosol Optical Depth (AOD) from instruments onboard the Terra and Aqua satellites (Remer et al., 2005; Davies et al., 2004) was also assimilated. A Mie code based look-up table of speciated aerosol mass extinction coefficients and relative humidity dependent hygroscopic growth factors is used to convert the predicted aerosol mass to speciated extinction, which is integrated vertically to obtain a first guess AOD for assimilation. The masses of all aerosol species are adjusted within each model layer on the basis of the total AOD analysis increment and the relative contribution of each aerosol species to the total layer extinction. The resulting RAQMS aerosol analysis is in good agreement with April 2008 global Aeronet measurements ($r = 0.7$, bias=0.05). During the chemical and aerosol assimilation cycle the RAQMS meteorological forecasts are reinitialized from NOAA Global Forecasting System (GFS) analyses at 6 h intervals.

3 Source identification of observed plumes

As discussed earlier, significant wild fires occurred in western Asia (Kazakhstan), eastern Asia (Siberia) and southeastern Asia (Thailand). Satellite fire counts over Russia were more than two times the April average in April 2008 (Fisher et al., 2010). Kazakhstan and Siberian fires are mainly due to burning of mixed coniferous and deciduous forest and croplands as observed by one-degree land cover derived from AVHRR.

Thailand fires are due to burning of broadleaf evergreen forest, grassland and cropland (http://glcf.umd.edu/data/landcover/).

3.1 RAQMS trajectory analysis

We use RAQMS chemical and aerosol analyses in conjunction with ensemble trajectory analysis (Pierce et al., 2009; Verma et al., 2009) to follow the chemical evolution of ensemble trajectories initialized at daily wildfire locations. The resulting Lagrangian photochemical histories of the wildfire plumes can be used to relate emissions from these biomass burning regions to the observed plumes. First, we look at the lower/middle tropospheric plume identified in Sect. 2.2.1 and detailed in Sect. 2.2.2. RAQMS forward wildfire trajectory analysis (left graph of Fig. 8) shows that the plume originates from Kazakhstan on the 7 April. This day was marked by a sudden increase of Kazakhstan fire CO emissions from less than 0.5 to more than 1.5 TgC day^{-1}. After initialization, ensemble trajectories are transported eastward, in the middle troposphere, over North Asia, across the Pacific via the Bering Sea and then south of Alaska where they are intersected by the NASA/DC8 flight track on the 19 April 2008, 12.5 days after initialization. During transport over Asia, the RAQMS model indicates that the wildfire plume was enhanced by Siberian biomass burning emissions with increase in CO and, carbonaneous aerosol (BCOC) (not shown in the figures). Moreover, the plume subsequently mixed with anthropogenic emissions over the Bering Sea, as indicated by increased SO_4 concentrations in RAQMS that is consistent with aircraft SO_2 measurement of approximately 700 pptv (Fig. 5).

The upper tropospheric plume (identified in Sect. 2.2.1) RAQMS forward wildfire trajectory analysis (right graph of Fig. 8) shows that the plume originates from Thailand on the 9 April. This date matches with high Thailand fire CO emissions up to 3.0 TgC day^{-1}, an intensity two times higher than the Kazakhstan fire. The plume was transported eastward over China and cross the Pacific along 40° N to reach NASA/DC8 flight track on the 19 April 2008, 10 days after emission.

Several studies (Bey et al., 2001; Jacob et al., 2003) have already shown that CO from biomass burning in Southeast Asia is transported over the Pacific by the particularly strong Asian outflow in spring. The frequent cyclogenesis off the coast of East Asia transport pollution to the free troposphere (Stohl, 2001; Liu et al., 2003; Miyazaki et al., 2003) where air masses are isolated from the surface. Then, plumes are transported to northern high latitudes and divided into northern and southern branches. The plume that originated from Thailand was transported over China and the RAQMS model suggested no enhancement by anthropogenic emissions.

Figure 9 shows a comparison between DIAL Aerosol Scattering Ratio (ASR) at the bottom and RAQMS carbonaceous aerosol mixing ratio from the baseline simulation at the top. The RAQMS baseline carbonaceous aerosol distribution along the DC8 flight curtain agrees spatially with the DIAL measurements and shows a major carbon aerosol enhancement in the lower troposphere (2–6 km) (up to 4.6 ppbv) and lower aerosol amounts in the upper troposphere (8–12 km) (up to 2.4 ppbv). RAQMS gives a realistic estimation of ozone concentrations in the troposphere but underestimates DIAL lower tropospheric ozone for the northern part of the flight (RAQMS max O_3 = 55 ppbv, DIAL max O_3 = 105 ppbv) (not shown in the figures). We use RAQMS sensitivity studies to quantify the impact of Asian biomass burning plumes on aerosols, O_3 and CO sampled by the DC8.

3.2 RAQMS O_3, CO and Carbonaceous Aerosols sensitivity study

We conducted a series of RAQMS simulations (without aerosol or ozone assimilation) where we restricted April 2008 wildfire emissions to within either the Kazakhstan, Siberian, or Thailand regions. Differences between the baseline RAQMS simulation and simulations with the restricted wildfire emissions are then used to infer which fires were primarily responsible for the aerosol and ozone enhancements observed by the DC8. Figure 10 shows RAQMS Carbonaceous aerosol (CC), CO and O_3 enhancements relative to background due to Asian fire emissions (Kazakhstan, Siberia and Thailand combined) and DIAL O_3 profiles along the DC8 flight 11. Based on this model

analysis, emissions from Kazakhstan, Baikal, and Thailand wildfires account for more than 90% of carbonaceous aerosols (CC) in the upper and lower/middle troposphere. However, upper tropospheric CC enhancements (2.2 ppbv) are two times less than lower/middle tropospheric enhancements (4.2 ppbv). On the other hand, upper tropospheric CO (dCO = 72 ppbv) and O_3 (dO_3 = 11 ppbv) enhancements are larger than lower tropospheric enhancements (dCO = 50 ppbv and dO_3 = 8.5 ppbv).

We also determined the impact of each fire on species concentrations along the profile but don't show the results. Kazakhstan wildfires account for the majority of lower tropospheric wildfire signatures with peak CC, CO and O_3 enhancements respectively of 3.4 ppbv, 33 ppbv and 5.5 ppbv. However, Siberian fires account for a small fraction of lower tropospheric wildfire signatures mostly below 2 km and at northern (60° N) part of DC8 flight. As seen before in Sect. 3.1, Kazakhstan fire trajectories overpass Siberian fires and entrain emissions from those fires. As a result, impacts on CO, CC and O_3 by Siberian fires are collocated with Kazakhstan fires dCC, dCO and dO_3.

As opposed to Kazakhstan and Siberian fires, Thailand fires have an impact on CC, CO and O_3 profiles in the upper troposphere. They account for the entire upper tropospheric fire signatures with peak CC, CO and O_3 enhancements of respectively 2.2 ppbv, 66 ppbv and 9.5 ppbv. The lower dCC/dCO ratios of the Thailand fires relative to the Kazakhstan fires is most likely due to stronger hydrophilic OC and BC losses within the Thailand plumes due to convective transport into the upper troposphere.

3.3 Ozone origin in Asian fire plumes

Using TES and RAQMS CO and O_3 profiles we observe and interpret CO and O_3 concentrations during transport of the Kazakhstan/Siberian and the Thailand plumes from emission to flight location. We also discuss the impact of fire emissions and stratospheric-tropospheric exchanges on O_3 concentrations.

3.3.1 Kazakhstan and Siberian fires

We next examine the Kazakhstan plume CO and O_3 concentrations at different locations during transport across the Pacific using the TES data and RAQMS chemical analyses. RAQMS ensemble trajectory analysis is used to determine which TES profiles sampled the wildfire plumes and we use TES and RAQMS CO and O_3 profiles to characterize the plume chemical and dynamical evolution. Table 1 shows dates, locations and UTC time of each TES wildfire plume profile used during the study.

Ozone and CO concentrations are examined in three locations as shown in Fig. 11a through Fig. 11c. First, we observe O_3 and CO concentrations in the plume on 7 April 2008 (YYYY/MM/DD) over source region (Kazakhstan). Then, we quantify plume evolution at an intermediate location over Siberian fires (14 April 2008). Finally, we determine plume O_3 and CO concentrations close to NASA/DC8 flight location and date (18 April 2008).

Tropospheric concentrations of CO are plotted against ozone using the TES observations over the Kazakhstan fire in the top left panel of Fig. 11a. Tropospheric CO and ozone concentrations from RAQMS chemical analysis are plotted in the bottom right panel of Fig. 11a. The bottom left panel shows these same RAQMS concentrations after the TES averaging kernel and constraint vector have been applied to account for the TES vertical sensitivity and retrieval bias (e.g., Jones et al., 2003; Pierce et al., 2009; Worden et al., 2004; Bowman et al., 2002, 2006, 2009). The CO/O_3 scatter plots are color-coded by the predicted CO enhancement associated with the Kazakhstan wildfires, as determined by the differences between the RAQMS baseline and no Kazakhstan wildfire emission simulations. Color-coding helps to indicate the impact of Kazakhstan fire emissions on RAQMS CO and O_3, and the same value are applied to TES observations. In all graphs, green to red points show high Kazakhstan fire influence on RAQMS CO concentrations.

Comparison of the bottom left panel of Fig. 11a to the upper left panel indicates that the RAQMS model estimates for maximum CO mixing ratios (~200 ppbv) agrees

well with the TES data after accounting for the vertical resolution and a priori of the TES data. However, comparison of the bottom left panel to the bottom right panel indicates that CO concentrations in the plume could be much larger (~700 ppbv) than observed by TES. The blue points indicate low fire influence on RAQMS CO concentrations. Comparison between the TES and the adjusted RAQMS model ozone (with TES operator) for these points indicates that RAQMS has lower background ozone in this region relative to TES. The negative correlation between O_3 and CO suggests that this air may have originated from the stratosphere. Therefore, for TES observations over Kazakhstan source region (Fig. 11a), elevated O_3 is mainly due to stratospheric enhancements and wildfire emissions do not result in significant O_3 enhancements within the plume. At this stage, O_3 concentrations in the plume are up to 60 ppbv, 10 ppbv over background level. This can be due to the fact that the plume sampling occurs right after plume emission and does not allow a sufficient time for O_3 precursors to react in the troposphere and produce O_3.

After emission, the Kazakhstan wildfire plume was transported eastward in the middle troposphere (~ 500hPa) over Asia. Before reaching the Pacific, the Kazakhstan plume encountered fire emissions from Siberia (Baikal) (Fig. 11b) leading to additional CO enhancements (up to 600 ppbv) that were not associated with the initial Kazakhstan emissions. TES and the adjusted RAQMS model agree in the estimation of maximum CO concentration (respectively 220 ppbv and 240 ppbv), but the adjusted RAQMS model is higher than TES CO concentrations by more than 70 ppbv. In the same way, the adjusted RAQMS model underestimates maximum O_3 concentrations observed by TES by more than 50 ppbv. In comparison, in Fig. 12, in situ measurements of O_3 onboard of the DC8 aircraft show higher concentrations with O_3 ranging from 60 to 120 ppbv with collocated CO over 150 ppbv (pink dots).

As suggested by the aircraft in situ SO_2 measurements (Sect. 2.2.2) and confirmed by the RAQMS analysis of the Lagrangian chemical evolution of the Kazakhstan wildfire plume, the plume mixed with Asian anthropogenic emissions. The plume was then transported in the middle troposphere over the Pacific via the Bering Sea and

reached flight location around the 18 April (Fig. 11c). Both TES and the adjusted RAQMS model show maximum CO concentrations (around 225 ppbv) and O_3 concentrations (max O_3 = 60 ppbv, min O_3 = 40 ppbv). However, lower CO concentrations are still overestimated by the adjusted RAQMS model by more than 60 ppbv and TES shows a low O_3 event, down to 20 ppbv of O_3, which is not captured by the adjusted RAQMS model. In situ measurements within the wildfire plume from flight 11 give O_3 concentrations ranging from 80 to 100 ppbv in the plume. Figure 12 shows that the RAQMS model significantly underestimates the dynamic range of in situ CO and O_3 (blue dots) along the DC8 flight track. RAQMS underestimates maximum in situ CO concentrations within the wildfire plume (yellow dots) and also underestimates ozone mixing ratios within the stratospheric intrusion sampled by the DC8 and observed in Fig. 3. Comparisons between RAQMS and in situ CO also suggests that RAQMS overestimates background CO by approximately 60 ppbv, which is consistent with the comparisons with TES in regions which were not strongly influenced by the Kazakhstan wildfire plume. Because of averaging across the tropopause, Investigation of TES and MODIS cloud data show that there is high cloud density over the region where the DC8 sample the main part of the plume. As a result, TES shows little sensitivity in O_3 between 50 and 60° N.

3.3.2 Thailand fires

Using the same approach as with the Kazakhstan fires, we examined the Thailand plume CO and O_3 concentrations at different locations during transport from the source and across the Pacific where the Thailand plume was eventually observed by DIAL on the DC8. Table 2 shows dates, locations and UTC time of each TES profiles used during the study.

In order to understand the plume's chemical and dynamical evolution, we use RAQMS simulation of CO and O_3 concentrations in the plume and compare it to TES observations. Three steps of the plume transport are discussed. First, we observe O_3 and CO concentrations in the plume immediately downwind of source region (Thailand)

during convective lifting over the Tibetan plateau (11 April 2008). Then, we quantify plume evolution at an intermediate location over the Pacific (15 April 2008) showing strong stratospheric air masses influence. Finally, we examine plume O_3 and CO concentrations near the NASA/DC8 flight location (19 April 2008).

Figure 13a, b and c show O_3 and CO concentrations comparisons as observed by RAQMS, the adjusted RAQMS model and TES at the three locations discussed above. In each figure, top right map gives the location of the plume and therefore of TES and RAQMS data. Bottom right, bottom left and top left graphs respectively show comparison between CO and O_3 concentrations in the plume from RAQMS, the adjusted RAQMS model, and TES.

As observed in the Kazakhstan/Siberian plume study, RAQMS CO downwind of source region (Fig. 13a) is higher than TES by almost a factor of 6 prior to applying the TES averaging kernel (AK) and a priori constraint. This discrepancy is due to the low sensitivity of the TES estimates to CO in the upper troposphere (Worden et al., 2004). However, after application the TES AK constraint to the RAQMS results, both ranges of variability of CO are in good agreement. As opposed to CO, the TES sensitivity is sufficient to resolve ozone variations in the middle and upper troposphere (e.g. Liu et al., 2009; Worden et al., 2009). Consequently, the TES and RAQMS ozone distributions are in better agreement prior to applying the TES AK.

Two days after plume emission (Fig. 13a), upper tropospheric O_3 concentrations observed by TES are likely due to stratospheric enhancement and photochemical O_3 produced from Thailand fires O_3 precursors. The color-coding shows that most of the plume is influenced by CO emissions from fires ($dCO > 150$ ppbv). However, for CO concentrations under 100 ppbv (TES) and dCO under 100 ppbv, we notice highest O_3 concentrations up to 240 ppbv for the adjusted RAQMS model and 320 ppbv for TES, due to exchange in stratospheric air into the troposphere. Indeed, as shown by Fig. 14, downwind of the Thailand fires, part of the Thailand plume is located in the upper troposphere over the Tibetan plateau where it is most likely to mix with stratospheric air masses. Top and middle profiles of Fig. 14 respectively show TES and adjusted

RAQMS model O_3 (left) and CO (right) concentrations. Bottom profiles of Fig. 14 show dO_3 and dCO concentration perturbations due the Thailand fires predicted by the RAQMS model. It allows a better representation of the plume position and elevation, and gives perturbations due to fires up to 60 ppbv of O_3 and 300 ppbv of CO. In Fig. 13a and b, O_3 enhancements are observed within the upper tropospheric portion of the Thailand plume with TES O_3 concentrations up to 120 ppbv. The adjusted RAQMS model is in good agreement with TES giving maximum O_3 concentrations up to 110 ppbv in this region of strong photochemical production.

The plume was then transported in the free troposphere over the Pacific. The distributions of CO and O_3 are shifted and show increased mixing between stratospheric and photochemically produced O_3. High fire influence (green to red points) leads to O_3 concentrations between 50 and 100 ppbv whereas stratospheric air masses (blue points) correspond to highest O_3 concentrations simulated by the adjusted RAQMS model (260 ppbv) and measured by TES (400 ppbv).

The plume reached the flight location on the 19 April. Along the flight track, TES and the adjusted RAQMS model give O_3 concentrations ranging from 50 to almost 420 ppbv. Lowest CO concentrations are collocated with highest O_3 concentrations around 400 ppbv for both TES and the adjusted RAQMS model. However, color-coding shows that emissions from Thailand fires also have an influence on those high O_3 concentrations. In summary, the RAQMS model (accounting for TES sensitivity) gives a good estimation of O_3 concentrations compared to TES but overestimates CO concentrations. Unfortunately, in situ measurements do not sample the upper tropospheric plume and therefore cannot be compared with the TES and RAQMS results.

4 Discussion

The combination of TES and RAQMS wildfire sensitivity experiments and ensemble wildfire trajectories allows us to localize both Kazakhstan/Siberian and Thailand plumes along their transport from Asia to NASA/DC8 flight location. Using those tools

allows us to understand chemical and dynamical evolution, and quantify the evolution of O_3 and CO concentrations within those plumes. In this next section we examine monthly mean dCO and dO_3 results from RAQMS.

Figure 15a and b show Kazakhstan and Siberian fires perturbations of CO (dCO) and O_3 (dO_3) in the troposphere during April 2008. Those fires contribute a maximum column density of 1.5×10^{18} molecules cm^{-2} of CO and 3 Dobson Unit (DU) of O_3. Highest impacts occur over Northern Asia but stretch eastward over the Pacific to reach Alaska and the Arctic. The plume's highest O_3 concentrations occur over Asia and then drop down as it reach the Pacific.

Figure 16a and b show Thailand fires perturbation of CO (dCO) and O_3 (dO_3) in the troposphere during April 2008. The most significant enhancements occur over South-Eastern Asia but stretch eastward over the Pacific to reach North America and even Europe and Africa. The Southeast Asian fires have a bigger impact on CO and O_3 in the troposphere than the Kazakhstan/Siberian fires. They contribute up to 3.0×10^{18} molecules cm^{-2} of CO and 10 Dobson Unit (DU) of O_3.

5 Conclusions

Using satellite ozone and CO tropospheric profile estimates from TES, and in situ and lidar data from the ARCTAS campaign, we explored the impact of Asian Boreal and Southeast Asian fires on tropospheric chemistry, long-range transport of associated pollutant over the Pacific and the chemical and dynamical processes influencing ozone concentrations.

On 19 April 2008, Differential Absorption Lidar (DIAL) onboard of NASA/DC8 aircraft sampled two major biomass burning plumes ashore of western North America. Real time Air Quality Modeling System (RAQMS) ensemble wildfire trajectory analysis showed that those plumes originated from Kazakhstan and Thailand where large wildfires were taking place with monthly mean CO emissions up to three times higher than usual April means. In situ measurements onboard the aircraft showed

high concentrations of CO, PAN, and BC consistent with biomass burning along with signatures of anthropogenic emissions (SO_2) and significant O_3 enhancements (up to 100 ppbv). RAQMS sensitivity studies allowed us to assess the relative impact of Asian fires on CO, O_3 and CC concentrations along DIAL profiles. It showed that Thailand fires were responsible for almost the entire biomass burning signature in the upper troposphere (8 to 12 km); whereas Kazakhstan and Siberian fires were responsible for the majority of the fire signature in the lower middle troposphere (2 to 6 km).

We examined CO and O_3 concentrations within these two distinct plumes using TES and RAQMS data and characterized the chemical evolution along their respective transport pathways. Over the Kazakhstan fire source region, the majority of O_3 observed by TES was due to stratospheric enhancement. Upon transport eastward in the middle troposphere (500 hPa) over Asia, the plume went over the Siberian fire and was exposed to additional CO and O_3 precursor enhancements. Finally, the plume crossed the Pacific over the Bering Sea and reached the flight location on the 19 April. Along the flight track, TES and RAQMS observe similar O_3 concentrations ranging from 40 to 60 ppbv. However, in situ measurements from flight 11 measured O_3 concentrations ranging from 80 to 100 ppbv in the plume; this increased ozone enhancement could be due to localized ozone production within narrow filaments of the wildfire plume that are not observed by TES due to its relatively broad weighting functions and not captured by RAQMS due to it's relatively coarse vertical and horizontal resolution.

The upper tropospheric plume, observed by DIAL, originated from Thailand in Southeast Asia. TES observations near the source indicate photochemical production of ozone in the plume along with uplift of the plume into the upper troposphere south of the Tibetan plateau. The plume mixed with stratospheric air resulting in further elevation of O_3 concentrations up to 300 ppbv. Then, the plume was transported in the middle/upper troposphere (mainly 100–400 hPa) over the Pacific. Along the flight track, on the 19 April, TES and the adjusted RAQMS model give O_3 concentrations ranging from 50 to almost 420 ppbv.

The relatively good agreement between RAQMS predictions and TES observations during the wildfire plume transport allows us to estimate how much ozone these fires produce. We find that on a monthly mean scale, the springtime Kazakhstan and Siberian fires increase ozone concentrations by 3 DU over source region and 1 DU over North America and that the Thailand fires increase ozone concentrations by approximately 10 DU over source region and 4 DU over North America. However, this estimate likely underestimates local ozone production based on comparisons between RAQMS and insitu DC8 measurements within the plume.

Considering this seasonal trend of biomass burning pollutant transport from Asia, it is important to characterize these events in order to understand their impact on air quality and climate. Recently, increase of CO by biomass burning in boreal area, and Southeast Asian fire emissions have been identified as affecting human health (Maynard and Waller, 1999) and perturbing atmospheric chemistry at regional and even global scales (Logan et al., 1981; Roths and Harris, 1996; Novelli et al., 1998; Bowman et al., 2009; Jones et al., 2009). Increases in population in Southeast Asia tend to increase burning of postharvest agricultural waste that is an important type of biomass burning in this region of the world (Crutzen and Andreae, 1990; Nguyen et al., 1994). Increased temperatures from global warming also tend to increase drought and decrease snow cover in Northern Asia leading to increases in fuel quantity and a longer fire season (Euskirchen et al., 2007).

Acknowledgements. The views, opinions, and findings contained in this report are those of the author(s) and should not be construed as an official National Oceanic and Atmospheric Administration or US Government position, policy, or decision.

References

Abel, S. J., Highwood, E. J., Haywood, J. M., and Stringer, M. A.: The direct radiative effect of biomass burning aerosols over southern Africa, Atmos. Chem. Phys., 5, 1999–2018, doi:10.5194/acp-5-1999-2005, 2005.

Al-Saadi, J. A., Soja, A., Pierce, R. B., Szykman, J., Wiedinmyer, C., Emmons, L., Kondragunta, S., Zhang, X. Y., Kittaka, C., Schaack, T., and Bowman, K.: Intercomparison of near-real-time biomass burning emissions estimates constrained by satellite fire data, J. Appl. Remote Sens., 2, 021504, doi:10.1117/1.2948785, 2008.

Andreae, M. O. and Merlet, P.: Emission of trace gases and aerosols from biomass burning, Global Biogeochem. Cy., 15, 955–966, doi:10.1029/2000GB001382, 2001.

Andreae, M. O.: Soot carbon and excess fine potassium – Long-range transport of combustion-derived aerosols, Science, 220(4602), 1148–1151, 1983.

Beer, R.: TES on the Aura Mission: Scientific objectives, measurements and analysis overview, IEEE T. Geosci. Remote, 44, 1102–1105, doi:10.1109/TGRS.2005.863716, 2006.

Beer, R., Glavich, T. A., and Rider, D. M.: Tropospheric emission spectrometer for the Earth Observing System's Aura satellite, Appl. Optics, 40, 2356–2367, doi:10.1364/AO.40.002356, 2001.

Bertschi, I. T. and Jaffe, D. A.: Long-range transport of ozone, carbon monoxide, and aerosols to the NE Pacific troposphere during the summer of 2003: Observations of smoke plumes from Asian boreal fires, J. Geophys. Res., 110, D05303, doi:10.1029/2004JD005135, 2005.

Bey, I., Jacob, D. J., Yantosca, R. M., Logan, J. A., Field, B. D., Fiore, A. M., Li, Q., Liu, H. Y., Mickley, L. J., and Schultz, M. G.: Global modeling of tropospheric chemistry with assimilated meteorology: Model description and evaluation, J. Geophys. Res., 106, 23073–23096, 2001.

Bian, H., Prather, M., and Takemura, T.: Tropospheric aerosol impacts on trace-gas budgets through photolysis, J. Geophys. Res., 108(D8), 4242, doi:10.1029/2002JD002743, 2003.

Bowman, K. W., Rodgers, C.D., Kulawik, S.S., Worden, J., Sarkissian, E., Osterman, G., Steck, T., Ming Lou, Eldering, A., Shephard, M., Worden, H., Lampel, M., Clough, S., Brown, P., Rinsland, C., Gunson, M. and Beer, R.: Tropospheric emission spectrometer: Retrieval method and error analysis, IEEE T. Geosci. Remote, 44, 1297–1307, doi:10.1109/TGRS.2006.871234, 2006.

Bowman, K. W., Jones, D. B. A., Logan, J. A., Worden, H., Boersma, F., Chang, R., Kulawik, S., Osterman, G., Hamer, P., and Worden, J.: The zonal structure of tropical O_3 and CO as observed by the Tropospheric Emission Spectrometer in November 2004 - Part 2: Impact of surface emissions on O_3 and its precursors, Atmos. Chem. Phys., 9, 3563–3582, doi:10.5194/acp-9-3563-2009, 2009.

Browell, E. V., Fenn, M. A., Butler, C. F., Grant, W. B., Ismail, S., Ferrare, R. A., Kooi, S. A., Brackett, V. G., Clayton, M. B., Avery, M. A., Barrick, J. D. W., Fuelberg, H. E., Maloney, J. C.,

Newell, R. E., Zhu, Y., Mahoney, M. J., Anderson, B. E., Blake, D. R., Brune, W. H., Heikes, B. G., Sachse, G. W., Singh, H. B., and Talbot, R. W.: Large-scale air mass characteristics observed over the remote tropical Pacific Ocean during March-April 1999: Results from PEM Tropics B Field Experiment, J. Geophys. Res., 106, 32481–32501, 2001.

Cahoon, D. R., Stocks Jr., B. J., Levine, J. S., Cofer III, W. R., and Pierson, J. M.: Satellite analysis of the severe 1987 forest fires in northern China and southeastern Siberia, J. Geophys. Res., 99, 18627–18638, 1994.

Chin, M., Ginoux, P., Kinne, S., Torres, O., Holben, B. N., Duncan, B. N., Martin, R. V., Logan, J. A., Higurashi, A., and Nakajima, T.: Tropospheric aerosol optical thickness from the GOCART model and comparisons with satellite and sunphotometer measurements, J. Atmos. Sci., 59, 461–483, doi:10.1175/1520-0469(2002), 2002.

Chin, M., Ginoux, P., Lucchesi, R., Huebert, B., Weber, R., Anderson, T., Masonis, S., Blomquist, B., Bandy, A., and Thornton, D.: A global aerosol model forecast for the ACE-Asia field experiment, J. Geophys. Res., 108(D23), 8654, doi:10.1029/2003JD003642, 2003.

Christopher, S. A., Chou, J., Welch, R. M., Kliche, D. V., and Connors, V. S.: Satellite investigations of fire, smoke, and carbon monoxide during April 1994 MAPS mission: Case studies over tropical Asia, J. Geophys. Res., 103, 19327–19336, 1998.

Cofer III, W. R., Levine, J. S., Winstead, E. L., and Stocks, B. J.: Trace gas and particulate emissions from biomass burning in temperate ecosystems, Global Biomass Burning: Atmospheric, Climatic, and Biospheric Implications, J. S. Levine, MIT Press, Cambridge, Mass., 203–208, 1991.

Conard, S. G., Sukhinin, A. I., Stocks, B. J., Cahoon, D. R., Davidenko, E. P., and Ivanova, G. A.: Determining effects of area burned and fire severity on carbon cycling and emissions in Siberia, Climate Change, 55(1–2), 197–211, 2002.

Crutzen, P. J. and Andreae, M. O.: Biomass burning in the tropics: Impact on atmospheric chemistry and biogeochemical cycles, Science, 250, 1669–1678.

Davies, D., Kumar, S., and Descloitres, J.: Global fire monitoring: Use of MODIS near-real-time satellite data, GIM International, 18(4), 41–43, 2004.

Dlugokencky, E. J., Walter, B. P., Masarie, K. A., Lang, P. M., and Kasischke, E. S.: Measurements of an anomalous global methane increase during 1998, Geophys. Res. Lett., 28(3), 499–502, 2001.

Eck, T. F., Holben, B. N., Ward, D. E., Mukelabai, M. M., Dubovik, O., Smirnov, A., Schafer, J. S., Hsu, N. C., Piketh, S. J., Queface, A., Le Roux, J., Swap, R. J., and Slutsker, I.:

Variability of biomass burning aerosol optical characteristics in southern Africa during the SAFARI 2000 dry season campaign and a comparison of single scattering albedo estimates from radiometric measurements, J. Geophys. Res., 108, 8477, doi:10.1029/2002JD002321, 2003.

Eckhardt, S., Stohl, A., Beirle, S., Spichtinger, N., James, P., Forster, C., Junker, C., Wagner, T., Platt, U., and Jennings, S. G.: The North Atlantic Oscillation controls air pollution transport to the Arctic, Atmos. Chem. Phys., 3, 1769–1778, doi:10.5194/acp-3-1769-2003, 2003.

Edwards, D. P., Emmons, L. K., Hauglustaine, D. A., Chu, D. A., Gille, J. C., Kaufman, Y. J., Petron, G., Yurganov, L. N., Giglio, L., Deeter, M. N., Yudin, V., Ziskin, D. C., Warner, J., Lamarque, J. F., Francis, G. L., Ho, S. P., Mao, D., Chen, J., Grechko, and E. I., Drummond, J. R.: Observations of carbon monoxide and aerosols from the Terra satellite: Northern Hemisphere variability, J. Geophys. Res., 109, D24202, doi:10.1029/2004JD004727, 2004.

Euskirchen, E. S., Mcguire, A. D., and Chapin, F. S.: Energy feedbacks of northern high-latitude ecosystems to the climate system due to reduced snow cover during 20th century warming, Glob. Change Biol., 13(11), 2425–2438, 2007.

Fisher, J. A., Jacob, D. J., Purdy, M. T., Kopacz, M., Le Sager, P., Carouge, C., Holmes, C. D., Yantosca, R. M., Batchelor, R. L., Strong, K., Diskin, G. S., Fuelberg, H. E., Holloway, J. S., Hyer, E. J., McMillan, W. W., Warner, J., Streets, D. G., Zhang, Q., Wang, Y., and Wu, S.: Source attribution and interannual variability of Arctic pollution in spring constrained by aircraft (ARCTAS, ARCPAC) and satellite (AIRS) observations of carbon monoxide, Atmos. Chem. Phys., 10, 977–996, doi:10.5194/acp-10-977-2010, 2010.

Fishman, J., Watson, C. E., Larsen, J. C. and Logan, J. A.: Distribution of tropospheric ozone determined from satellite data, J. Geosphy. Res., 95, 3599–3617, 1990.

Forster, C., Wandinger, U., Wotawa, G., James, P., Mattis, I., Althausen, D., Simmonds, P., O'Doherty, S., Jennings, S. G., Kleefeld, C., Schneider, J., Trickl, T., Kreipl, S., Jager, H., and Stohl, A.: Transport of boreal forest fire emissions from Canada to Europe, J. Geophys. Res., 106, 22887–22906, doi:10.1029/2001JD900115, 2001.

Fromm, M., Alfred, J., Hoppel, K., Hornstein, J., Bevilacqua, R., Shettle, E., Servranckx, R., Li, Z. Q., and Stocks, B.: Observations of boreal forest fire smoke in the stratosphere by POAM III, SAGE II, and lidar in 1998, Geophys. Res. Let., 27(9), 1407–1410, 2000.

Goloub, P. and Arino, O.: Verification of the consistency of Polder Aerosol Index over land with ATSR-2/ERS-2 fire product, Geophys. Res. Lett., 27, 899–902, 2000.

Haines, D. A.: A lower atmosphere severity index for wildland fires, Natl. Weather Dig., 13,

23–27, 1988.

Hao, W. M. and Ward, D. E.: Methane production from global biomass burning, J. Geophys. Res., 98, 20657–20661, 1993.

Haywood, J. and Boucher, O.: Estimates of the direct and indirect radiative forcing due to tropospheric aerosols: A review, Rev. Geophys., 38(4), 513–543, 2000.

Heald, C. L., Daniel, J. J., Arlene, M. F., Louisa, K. E., John, C. G., Merritt, N. D., Juying, W., David, P. E., James, H. C., Amy, J. H., Glen, W. S., Edward, V. B., Melody, A. A., Stephanie, A. V., David, J. W., Donald, R. B., Hanwant, B. S., Scott, T. S., Robert, W. T., and Fuelberg, H. E.: Asian outflow and trans- Pacific transport of carbon monoxide and ozone pollution: An integrated satellite, aircraft, and model perspective, J. Geophys. Res., 108(D24), 4804, doi:10.1029/2003JD003507, 2003.

Jacob, D. J., Crawford, J. H., Kleb, M. M., Connors, V. S., Bendura, R. J., Raper, J. L., Sachse, G. W., Gille, J. C., Emmons, L., and Heald, C. L.: Transport and Chemical Evolution over the Pacific (TRACE-P) aircraft mission: Design, execution, and first results, J. Geophys. Res., 108(D20), 9000, doi:10.1029/2002JD003276, 2003.

Jacob, D. J., Crawford, J. H., Maring, H., Clarke, A. D., Dibb, J. E., Emmons, L. K., Ferrare, R. A., Hostetler, C. A., Russell, P. B., Singh, H. B., Thompson, A. M., Shaw, G. E., McCauley, E., Pederson, J. R., and Fisher, J. A.: The Arctic Research of the Composition of the Troposphere from Aircraft and Satellites (ARCTAS) mission: design, execution, and first results, Atmos. Chem. Phys., 10, 5191–5212, doi:10.5194/acp-10-5191-2010, 2010.

Jaffe, D., Mahula, A., Kelley, J., Atkins, J., Novelli, P. C., and Merrill, J.: Impact of Asian emissions on the remote North Pacific atmosphere: Interpretation of CO data from Shemya, Guam, Midway and Mauna Loa, J. Geophys. Res., 102, 28627–28635, 1997.

Jaffe, D., Bertschi, I., Jaegle, L., Novelli, P., Reid, J. S., Tanimoto, H., Vingarzan, R., and Westphal, D. L.: Long-range transport of Siberian biomass burning emissions and impact on surface ozone in western North America, Geophys. Res. Lett., 31, L16106, doi:10.1029/2004GL020093, 2004.

Jones, D. B. A., Bowman, K. W., Logan, J. A., Heald, C. L., Liu, J., Luo, M., Worden, J., and Drummond, J.: The zonal structure of tropical O_3 and CO as observed by the Tropospheric Emission Spectrometer in November 2004 - Part 1: Inverse modeling of CO emissions, Atmos. Chem. Phys., 9, 3547–3562, doi:10.5194/acp-9-3547-2009, 2009.

Kajii, Y., Kato, S., Streets, D. G., Tsai, N. Y., Shvidenko, A., Nilsson, S., McCallum, I., Minko, N. P., Abushenko, N., Altyntsev, D., and Khodzer, T. V.: Boreal forest fires in Siberia in 1998:

Estimation of area burned and emissions of pollutants by advanced very high resolution radiometer satellite data, J. Geophys. Res., 107(D24), 4745, doi:10.1029/2001JD001078, 2002.

Kasischke, E. S. and Bruhwiler, L. P.: Emissions of carbon dioxide, carbon monoxide, and methane from boreal forest fires in 1998, J. Geosphy. Res., 108(8146), doi:10.1029/2001JD000461, 2002.

Kasischke, E. S., Hyer, E. J., Novelli, P. C., Bruhwiler, L. P., French, N. H. F., Sukhinin, A. I., Hewson, J. H., and Stocks, B. J.: Influence of boreal fire emissions on Northern Hemisphere atmospheric carbon and carbon monoxide, Global Biogeochem. Cy., 19, GB1012, doi:10.1029/2004GB002300, 2005.

Kato, S., Pochanart, P., Hirokawa, J., Kajii, Y., Akimoto, H., Ozaki, Y., Obi, K., Katsuno, T., Streets, D. G., and Minko, N. P.: The influence of Siberian forest fires on carbon monoxide concentrations at Happo, Japan, Atmos. Environ., 36, 385–390, 2002.

Kittaka, C., Pierce, R. B., Crawford, J. H., Hitchman, M. H., Johnson, D. R., Tripoli, G. J., Chin, M., Bandy, A. R., Weber, R. J., Talbot, R. W., and Anderson, B. E.: A three-dimensional regional modeling study of the impact of clouds on sulfate distributions during TRACE-P, J. Geophys. Res., 109, D15S11, doi:10.1029/2003JD004353, 2004.

Klonecki, A., Hess, P., Emmons, L., Smith, L., Orlando, J. and Blake, D.: Seasonal changes in the transport of pollutants into the Arctic troposphere-model study, J. Geophys. Res., 108, 8367, doi:10.1029/2002JD002199, 2003.

Koch, D. and Hansen, J.: Distant origins of Arctic black carbon: A Goddard Institute for Space Studies ModelE experiment, J. Geophys. Res., 110, D04204, doi:10.1029/2004JD004620, 2005.

Lapina, K., Honrath, R. E., Owen, R. C., Val Martin, M., and Pfister, G.: Evidence of significant large-scale impacts of boreal fires on ozone levels in the midlatitude Northern Hemisphere free troposphere, Geophys. Res. Lett., 33, L10815, doi:10.1029/2006GL025878, 2006.

Liang, Q., Jaegle, L., Jaffe, D. A., Weiss-Penzias, P., Heckman, A., and Snow, J. A.: Long-range transport of Asian pollution to the northeast Pacific: Seasonal variations and transport pathways of carbon monoxide, J. Geophys. Res., 109, D23S07, doi:10.1029/2003JD004402, 2004.

Liu, H., Jacob, D. J., Bey, I., Yantosca, R. M., Duncan, B. N., and Sachse, G. W.: Transport pathways for Asian pollution outflow over the Pacific: Interannual and seasonal variations, J. Geophys. Res., 108(D20), 8786, doi:10.1029/2002JD003102, 2003.

Liu, J. J., Jones, D. B. A., Worden, J. R., Noone, D., Parrington, M., and Kar, J.: Analysis of the summertime buildup of tropospheric ozone abundances over the Middle East and North Africa as observed by the Tropospheric Emission Spectrometer instrument, J. Geophys. Res., 114, D05304, doi:10.1029/2008JD010993, 2009.

Logan, J. A., Prather, M. J., Wofsy, S. C., and McElroy, M. B.: Tropospheric Chemistry: A Global Perspective, J. Geophys. Res., 86(C8), 7210–7254, 1981.

Massie, S. T., Torres, O., and Smith, S. J.: Total Ozone Mapping Spectrometer (TOMS) observations of increases in Asian aerosol in winter from 1979 to 2000, J. Geophys. Res.-Atmos., 109, D18211, doi:10.1029/2004JD005296, 2004.

Mauzerall, D. L., Jacob, D. J., Fan, S. M., Bradshaw, J. D., Gregory, G. L., Sachse, G. W., and Blake, D. R.: Origin of tropospheric ozone at remote high northern latitudes in summer, J. Geophys. Res., 101, 4175–4188, doi:10.1029/95JD03224, 1996.

Mauzerall, D. L., Logan, J. A., Jacob, D. J., Anderson, B. E., Blake, D. R., Bradshaw, J. D., Heikes, B., Sachse, G. W., Singh, H., and Talbot, B.: Photochemistry in biomass burning plumes and implications for tropospheric ozone over the tropical South Atlantic, J. Geophys. Res.-Atmos., 103, 8401–8423, 1998.

Maynard, R. L. and Waller, R.: Carbon monoxide, Air Pollution and health, edited by: Holgate, S. T., Samet, J. M., Koren, H.S. and Maynard, R.L, Academic, San Diego, Calif., 749–796, 1999.

Morris, G. A., Hersey, S., Thompson, A. M., Pawson, S., Nielsen, J. E., Colarco, P. R., McMillan, W. W., Stohl, A., Turquety, S., Warner, J., Johnson, B. J., Kucsera, T. L., Larko, D. E., Oltmans, S. J., and Witte, J. C.: Alaskan and Canadian forest fires exacerbate ozone pollution over Houston, Texas, on 19 and 20 July 2004, J. Geophys. Res., 111, D24S03, doi:10.1029/2006JD007090, 2006.

Myhre, G., Berntsen, T. K., Haywood, J. M., Sundet, J. K., Holben, B. N., Johnsrud, M., and Stordal, F.: Modeling the solar radiative impact of aerosols from biomass burning during the Southern African Regional Science Initiative (SAFARI-2000) experiment, J. Geophys. Res., 108, 8501, doi:10.1029/2002JD002313, 2003.

Nassar, R., Logan, J. A., Worden, H., Megretskaia, I. A., Bowman, K. W., Osterman, G., Thompson, A. M., Tarasick, D. W., Austin, S., Claude, H., Dubey, M. K., Hocking, W. K., Johnson, B. J., Joseph, E., Merrill, J., Morris, G. A., Newchurch, M., Oltmans, S. J., Posny, F., Schmidlin, F. J., Vomel, H., Whiteman, D. N., and Witte, J. C.: Validation of Tropospheric Emission Spectrometer (TES) nadir ozone profiles using ozonesonde measurements, J. Geophys.

Res., 113, D15S17, doi:10.1029/2007JD008819, 2008.
Nedelec, P., Thouret, V., Brioude, J., Sauvage, B., Cammas, J.-P., and Stohl, A.: Extreme CO concentrations in the upper troposphere over northeast Asia in June 2003 from the in situ MOZAIC aircraft data, Geophys. Res. Lett., 32, L14807, doi:10.1029/2005GL023141, 2005.
Nguyen, B. C., Mihalopoulos, N., and Putaud, J.-P.: Rice straw burning in Southeast Asia as a source of CO and COS to the atmosphere, J. Geophys. Res., 99, 16435–16439, 1994.
Novelli, P. C., Masarie, K. A., and Lang, P. M.: Distributions and recent changes of carbon monoxide in the lower troposphere, J. Geophys. Res., 103, 19015–19033, 1998.
Novelli, P. C., Masarie, K. A., Lang, P. M., Hall, B. D., Myers, R. C., and Elkins, J. W.: Reanalysis of tropospheric CO trends: Effects of the 1997–1998 wildfires, J. Geophys. Res., 108(D15), 4464, doi:10.1029/2002JD003031, 2003.
Osterman, G., Bowman, K., Eldering, A., Kulawik, S., Worden, J. et al.: Tropospheric emission spectrometer (TES) validation report, version 1.00, Internal Rep. D-33192, Jet Propul. Lab., Pasadena, Calif., 2005.
Pfister, G., Hess, P. G., Emmons, L. K., Lamarque, J.-F., Wiedinmyer, C., Edwards, D. P., Petron, G., Gille, J. C., and Sachse, G. W.: Quantifying CO emissions from the 2004 Alaskan wildfires using MOPITT CO data, Geophys. Res. Lett., 32, L11809, doi:10.1029/2005GL022995, 2005.
Pierce, R. B., Al-Saadi, J. A., Schaack, T., Lenzen, A., Zapotocny, T., Johnson, D., Kittaka, C., Buker, M., Hitchman, M. H., Tripoli, G., Fairlie, T. D., Olson, J. R., Natarajan, M., Crawford, J., Fishman, J., Avery, M., Browell, E. V., Creilson, J., Kondo, Y., and Sandholm, S. T.: Regional Air Quality Modeling System (RAQMS) predictions of the tropospheric ozone budget over east Asia, J. Geophys. Res., 108(D21), 8825, doi:10.1029/2002JD003176, 2003.
Pierce, R. B., Schaack, T., Al-Saadi, J. A., Fairlie, T. D., Kittaka, C., Lingenfelser, G., Natarajan, M., Olson, J., Soja, A., Zapotocny, T., Lenzen, A., Stobie, J., Johnson, D., Avery, M. A., Sachse, G. W., Thompson, A., Cohen, R., Dibb, J. E., Crawford, J., Rault, D., Martin, R., Szykman, J., and Fishman, J.: Chemical data assimilation estimates of continental US ozone and nitrogen budgets during the Intercontinental Chemical Transport Experiment-North America, J. Geophys. Res., 112, D12S21, doi:10.1029/2006JD007722, 2007.
Pierce, R. B., Al-Saadi, J., Kittaka, C., Schaack, T., Lenzen, A., Bowman, K., Szykman, J., Soja, A., Ryerson, T., Thompson, A. M., Bhartia, P., and Morris, G. A.: Impacts of background ozone production on Houston and Dallas, Texas, air quality during the Second Texas Air Quality Study field mission, J. Geophys. Res.-Atmos., 114, D00F09,

doi:10.1029/2008JD011337, 2009.
Pochanart, P., Akimoto, H., Kajii, Y., and Sukasem, P.: Carbon monoxide, regional-scale transport, and biomass burning in tropical continental Southeast Asia: Observations in rural Thailand, J. Geophys. Res., 108(D17), 4552, doi:10.1029/2002JD003360, 2003.
Quinn, P. K., Shaw, G., Andrews, E., Dutton, E. G., Ruoho-Airola, T., and Gong, S. L.: Arctic haze: current trends and knowledge gaps, Tellus B, 59, 99–114, doi:10.1111/j.1600-0889.2006.00238.x, 2007.
Real, E., Law, K. S., Weinzierl, B., Fiebig, M., Petzold, A., Wild, O., Methven, J., Arnold, S., Stohl, A., Huntrieser, H., Roiger, A., Schlager, H., Stewart, D., Avery, M., Sachse, G., Browell, E., Ferrare, R., and Blake, D.: Processes influencing ozone levels in Alaskan forest fire plumes during long-range transport over the North Atlantic, J. Geophys. Res., 112, D10S41, doi:10.1029/2006JD007576, 2007
Reichle, H. G., Connors, V. S., Holland, J. A., Hypes, W. D., Wallio, H. A., Casas, J. C., Gormsen, B. B., and Saylor, M. S.: Middle and upper tropospheric carbon-monoxide mixing ratios as measured by satellite-borne remote sensor during November 1981, J. Geophys. Res., 91, 865–887, 1986.
Reid, J. S., Koppmann, R., Eck, T. F., and Eleuterio, D. P.: A review of biomass burning emissions part II: intensive physical properties of biomass burning particles, Atmos. Chem. Phys., 5, 799–825, doi:10.5194/acp-5-799-2005, 2005.
Reid, J. S., Eck, T. F., Christopher, S. A., Koppmann, R., Dubovik, O., Eleuterio, D. P., Holben, B. N., Reid, E. A., and Zhang, J.: A review of biomass burning emissions part III: intensive optical properties of biomass burning particles, Atmos. Chem. Phys., 5, 827–849, doi:10.5194/acp-5-827-2005, 2005.
Remer, L. A., Kaufman, Y. J., Tanre', D., Mattoo, S., Chu, D. A., Martins, J. V., Li, R.-R., Ichoku, C., Levy, R. C., Kleidman, R. G., Eck, T. F., and Vermote, E.: The MODIS aerosol algorithm, products and validation, J. Atmos. Sci., 62, 947–973, doi:10.1175/JAS3385.1, 2005.
Richards, N. A. D., Li, Q. B., Osterman, G. B., Browell, E. V., Avery, M., and Bowman, K. W.: Validation of Tropospheric Emission Spectrometer (TES) measurements of the total, stratospheric, and tropospheric column abundance of ozone, J. Geophys. Res., 113, D15S16, doi:10.1029/2007JD008801, 2008.
Roths, J. and Harris, G. W.: The tropospheric distribution of carbon monoxide as observed during the Tropoz II Experiment, J. Atmos. Chem., 24, 157–188, 1996.
Seiler, W. and Crutzen, P. J.: Estimates of gross and net fluxes of carbon between the biosphere

and the atmosphere from biomass burning, Climate Change, 2(3), 207–247, 1980.
Shaw, G. E.: The arctic haze phenomenon, B. Am. Meteor. Soc., 76, 2403–2413, 1995.
Shindell, D. T., Chin, M., Dentener, F., Doherty, R. M., Faluvegi, G., Fiore, A. M., Hess, P., Koch, D. M., MacKenzie, I. A., Sanderson, M. G., Schultz, M. G., Schulz, M., Stevenson, D. S., Teich, H., Textor, C., Wild, O., Bergmann, D. J., Bey, I., Bian, H., Cuvelier, C., Duncan, B. N., Folberth, G., Horowitz, L. W., Jonson, J., Kaminski, J. W., Marmer, E., Park, R., Pringle, K. J., Schroeder, S., Szopa, S., Takemura, T., Zeng, G., Keating, T. J., and Zuber, A.: A multi-model assessment of pollution transport to the Arctic, Atmos. Chem. Phys., 8, 5353–5372, doi:10.5194/acp-8-5353-2008, 2008.
Simmonds, P. G., Manning, A. J., Derwent, R. G., Ciais, P., Ramonet, M., Kazan, V., and Ryall, D.: A burning question: Can recent growth rate anomalies in the greenhouse gases be attributed to large-scale biomass burning events?, Atmos. Environ., 39, 2513–2517, doi:10.1016/j.atmosenv.2005.02.018, 2005.
Singh, H. B. and Hanst, P. L.: Peroxyacetyl Nitrate (PAN) in the unpolluted atmosphere – an important reservoir for Nitrogen-Oxides, Geophy. Res. Lett., 8(8), 941–944, 1981.
Soja, A. J., Cofer, W. R., Shugart, H. H., Sukhinin, A. I., Stackhouse, P. W., McRae, D. J., and Conard, S. G.: Estimating fire emissions and disparities in boreal Siberia (1998–2002), J. Geophys. Res.-Atmos., 109, D14S06, doi:10.1029/2004JD004570, 2004.
Soja, A. J., Tchebakova, N. M., French, N. H. F., Flannigan, M. D., Shugart, H. H., Stocks, B. J., Sukhinin, A. I., Parfenova, E. I., Chapin, F. S., and Stackhouse, P. W.: Climate-induced boreal forest change: Predictions vs. current observations, Glob. Planet Change, 56(3–4), 274–296, 2007.
Staudt, A. C., Jacob, D. J., Logan, J. A., Bachiochi, D., Krishnamurti, T. N., and Sachse, G. W.: Continental sources, transoceanic transport, and interhemispheric exchange of carbon monoxide over the Pacific, J. Geophys. Res., 106(D23), 32571–32590, 2001.
Stohl, A.: Characteristics of atmospheric transport into the Arctic troposphere, J. Geophys. Res., 111, D11306, doi:10.1029/2005JD006888, 2006.
Tanimoto, H., Kajii, Y., Hirokawa, J., Akimoto, H., and Minko, N. P.: The atmospheric impact of boreal forest fires in far eastern Siberia on the seasonal variation of carbon monoxide: Observations at Rishiri, a northern remote island in Japan, Geophys. Res. Lett., 27, 4073–4076, 2000.
Thompson, A. M., Hogan, K. B., and Hoffman, J. S.: Methane reductions – Implications for global warming and atmospheric chemical-change, Atmos. Environ., 26(14), 2665–2668,

1992.
Turquety, S., Clerbaux, C., Law, K., Coheur, P.-F., Cozic, A., Szopa, S., Hauglustaine, D. A., Hadji-Lazaro, J., Gloudemans, A. M. S., Schrijver, H., Boone, C. D., Bernath, P. F., and Edwards, D. P.: CO emission and export from Asia: an analysis combining complementary satellite measurements (MOPITT, SCIAMACHY and ACE-FTS) with global modeling, Atmos. Chem. Phys., 8, 5187–5204, doi:10.5194/acp-8-5187-2008, 2008.
val Martin, M., Honrath, R., Owen, R. C., Pfister, G., Fialho, P., and Barata, F.: Significant enhancements of nitrogen oxides, ozone and aerosol black carbon in the North Atlantic lower free troposphere resulting from North American boreal wildfires, J. Geophys. Res., 111, D23S60, doi:10.1029/2006JD007530, 2006.
Reid, J. S., Eck, T. F., Christopher, S. A., Koppmann, R., Dubovik, O., Eleuterio, D. P., Holben, B. N., Reid, E. A., and Zhang, J.: A review of biomass burning emissions part III: intensive optical properties of biomass burning particles, Atmos. Chem. Phys., 5, 827–849, doi:10.5194/acp-5-827-2005, 2005.
Verma, S., Worden, J. R., Pierce, R. B., Jones, D. B. A., Al-Saadi, J., Boersma, F., Bowman, K., Eldering, A., Fisher, B., Jourdain, L., Kulawik, S. and Worden, H.: Ozone production in boreal fire smoke plumes using observations from the Tropospheric Emission Spectrometer and the Ozone Monitoring Instrument, J. Geophys. Res., 114, D02303, doi:10.1029/2008JD010108, 2009.
Warneke, C., Bahreini, R., Brioude, J., Brock, C. A., de Gouw, J. A., Fahey, D. W., Froyd, K. D., Holloway, J. S., Middlebrook, A., Miller, L., Montzka, S., Murphy, D. M., Peischl, J., Ryerson, T. B., Schwarz, J. P., Spackman, J. R., and Veres, P.: Biomass burning in Siberia and Kazakhstan as an important source for haze over the Alaskan Arctic in April 2008, Geophys. Res. Lett., 36, L02813, doi:10.1029/2008gl036194, 2009.
Worden, J., Kulawik, S. S. , Shephard, M. W., Clough, S. A., Worden, H., Bowman, K., and Goldman, A.: Predicted errors of tropospheric emission spectrometer nadir retrievals from spectral window selection, J. Geophys. Res., 109, D09308, doi:10.1029/2004JD004522, 2004.
Worden, H. M., Logan, J. A., Worden, J. R., Beer, R., Bowman, K., Clough, S. A., Eldering, A., Fisher, B. M., Gunson, M. R., Herman, R. L., Kulawik, S. S., Lampel, M. C., Luo, M., Megretskaia, I. A., Osterman, G. B., and Shephard, M. W.: Comparisons of Tropospheric Emission Spectrometer (TES) ozone profiles to ozonesondes: Methods and initial results, J. Geophys. Res., 112, D03309, doi:10.1029/2006JD007258, 2007.

Wotawa, G. and Trainer, M.: The influence of Canadian forest fires on pollutant concentrations in the United States, Science, 288(5464), 324–328, doi:10.1126/science.288.5464.324, 2000.

Yashiro, H., Sugawara, S., Sudo, K., Aoki, S., and Nakazawa, T.: Temporal and spatial variations of carbon monoxide over the western part of the Pacific Ocean, J. Geophys. Res., 114, D08305, doi:10.1029/2008jd010876, 2009.

Yurganov, L. N., Jaffe, D. A., Pullman, E., and Novelli, P. C.: Total column and surface densities of atmospheric carbon monoxide in Alaska, 1995, J. Geophys. Res., 103, 19337–19345, 1998.

Zhao, T. X. P., Stowe, L. L., Smirnov, A., Crosby, D., Sapper, J., and McClain, C. R.: Development of a global validation package for satellite oceanic aerosol optical thickness retrieval based on AERONET observations and its application to NOAA/NESDIS operational aerosol retrievals, J. Atmos. Sci., 59(3), 294–312, 2002.

Table 1. Dates, locations and UTC time of each TES profile used during the Kazakhstan/Siberian wildfire plume study.

Date	Mean latitude	Mean longitude	UTC time
7 April 2008	56° N	85° E	20:45
10 April 2008	55° N	100–105° E	06:05
11 April 2008	50° N	115° E	18:40
12 April 2008	52° N	130° E	04:15
14 April 2008	52° N	135–140° E	04:00
16 April 2008	55° N	175–180° W	00:30
16 April 2008	55° N	160–165° W	23:30
17 April 2008	57° N	155° W	13:00
18 April 2008	55° N	150° W	23:25

Table 2. Dates, locations and UTC time of each TES profile used during the Thailand wildfire plume study.

Date	Mean latitude	Mean longitude	UTC time
9 April 2008	24.3	98.8° E	06:50
10 April 2008	28	101° E	06:35
11 April 2008	27.1	108.1° E	18:00
12 April 2008	34.8	116.3° E	04:45
14 April 2008	34.6	127.1° E	05:00
15 April 2008	40.1	167.4° E	15:00
17 April 2008	54.1	170.5° W	13:00
19 April 2008	57.4	144.3° W	11:00

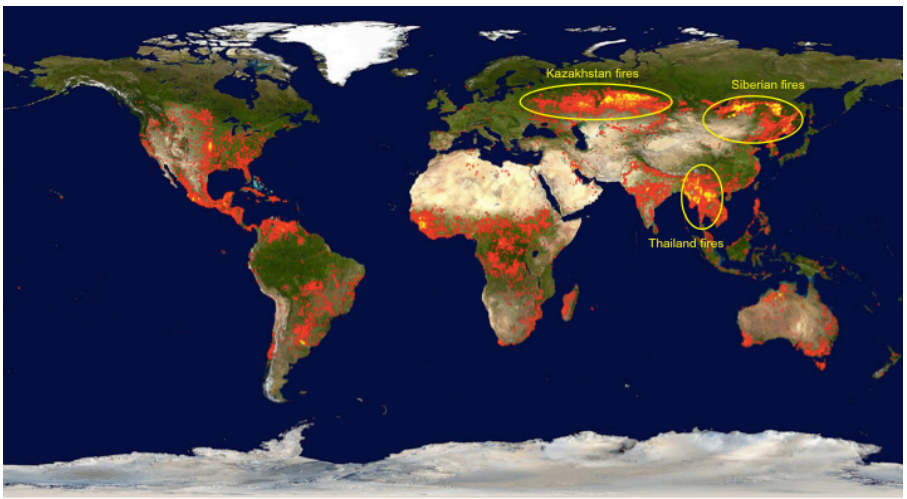

Fig. 1. April 2008 MODIS fire count.

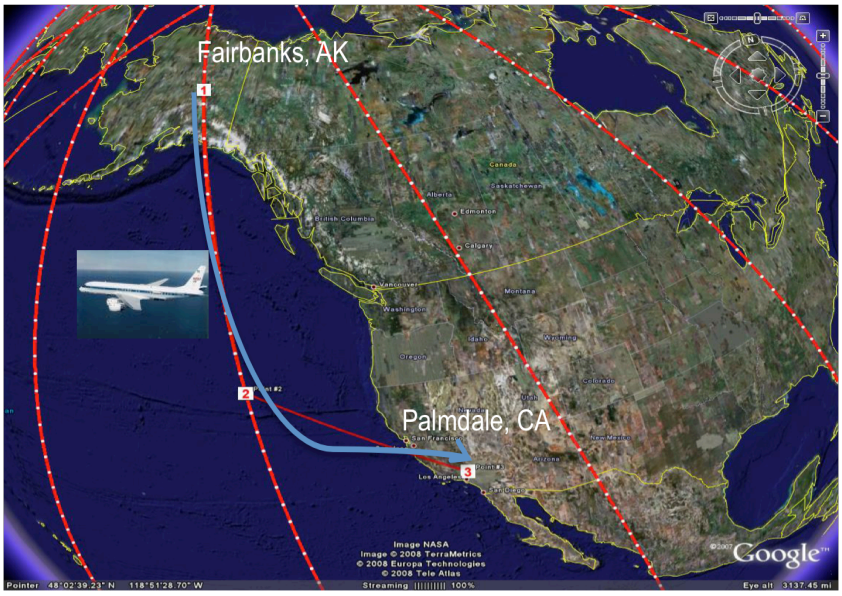

Fig. 2. Flight 11 (19 April 2008) track.

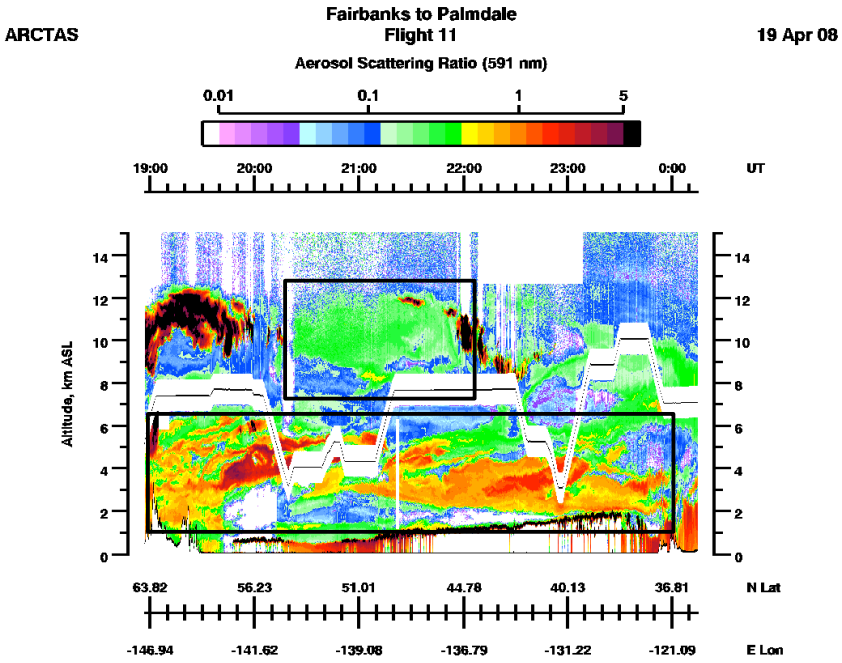

Fig. 3. Aerosol Scattering Ratio (ASR) from the Differential Analysis Lidar during DC8 flight 11 and square limiting aerosol plumes.

Discussion Paper | Discussion Paper | Discussion Paper | Discussion Paper |

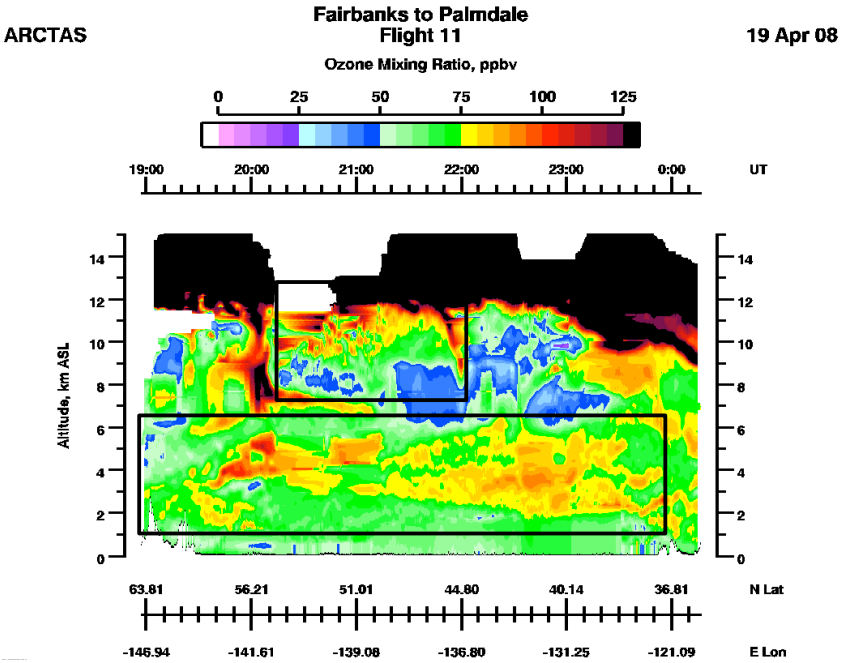

Fig. 4. Differential Analysis Lidar ozone (O_3) mixing ratio and square limiting two ozone plumes.

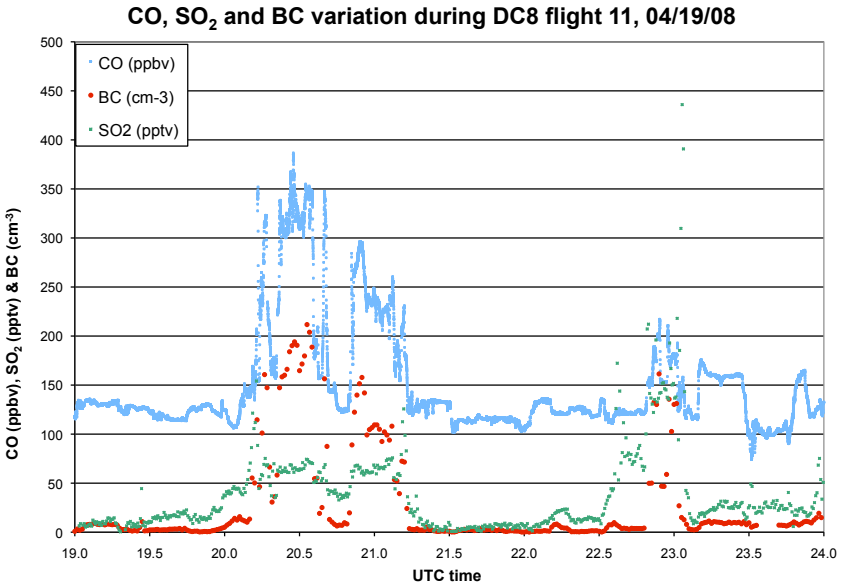

Fig. 5. Carbon monoxide (CO) (blue dots), sulfur dioxide (SO_2) (green dots) and Black Carbon (BC) (red dots) in situ measurement during DC8 flight 11 as a function of UTC time.

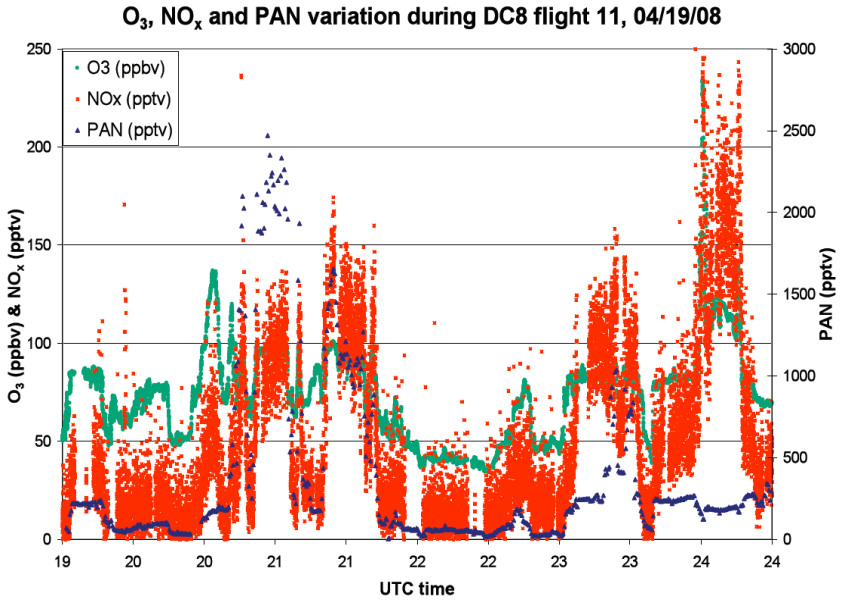

Fig. 6. Ozone (O_3) (green dots), Nitrogen Oxides (NO_x) (red dots) and Peroxyacetyl Nitrate (PAN) (blue dots) in situ measurement during DC8 flight 11 as a function of UTC time.

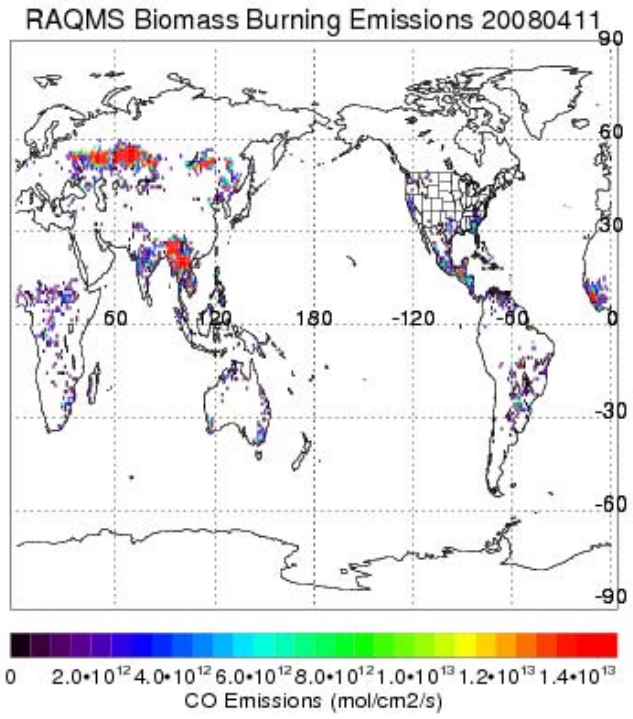

Fig. 7. Biomass burning Carbon monoxide (CO) emissions from RAQMS.

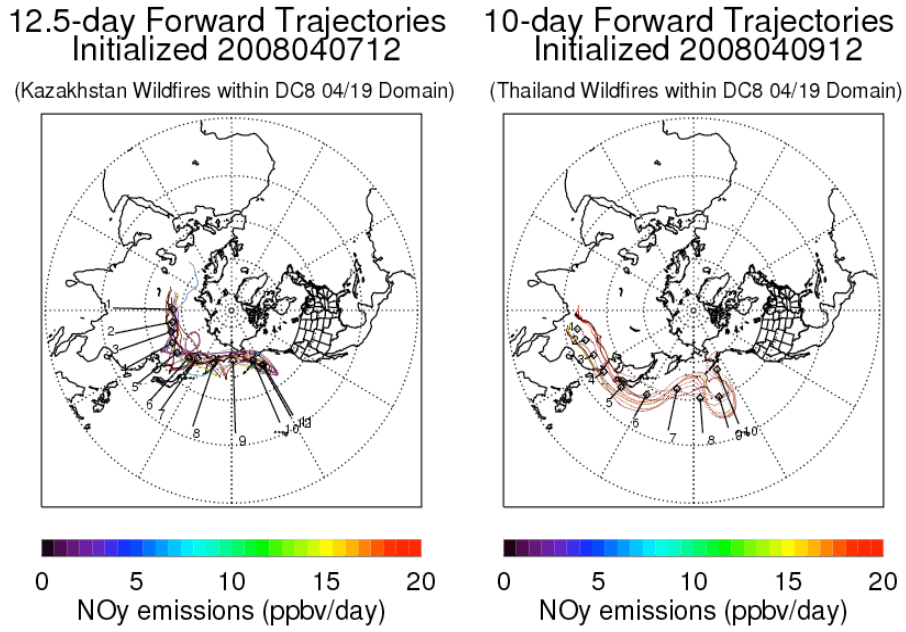

Fig. 8. Lower/middle and upper tropospheric plumes RAQMS trajectory analysis.

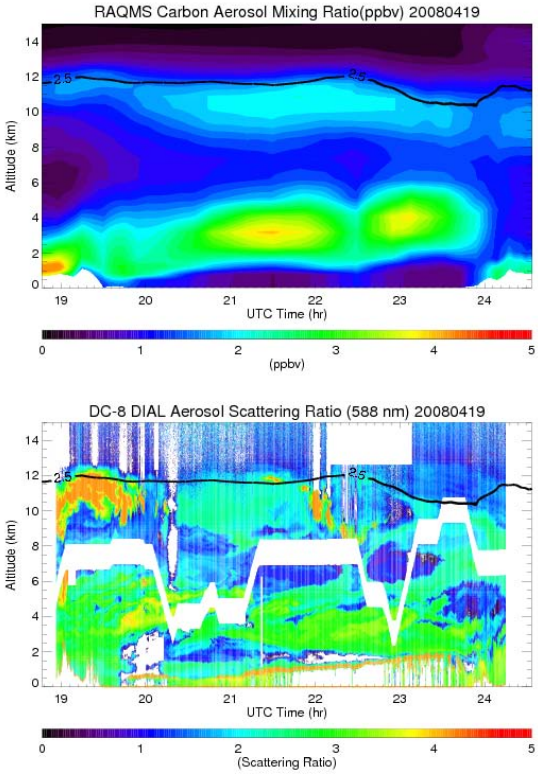

Fig. 9. Comparison between RAQMS carbonaceous aerosol (CC) profile (top) and DIAL Aerosol Scattering Ratio (ASR) (bottom) along DC8/NASA flight 11.

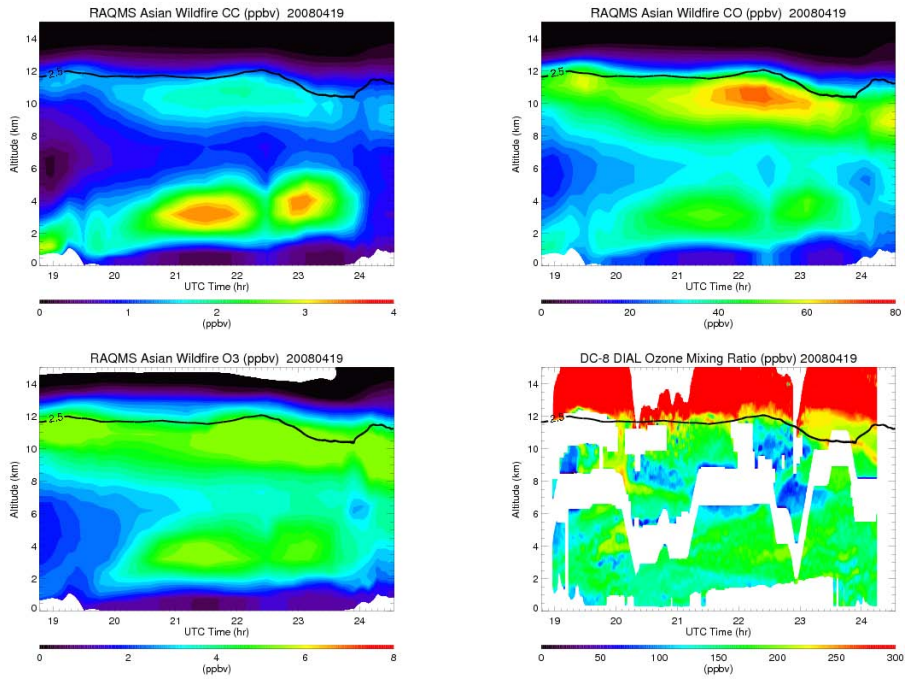

Fig. 10. RAQMS carbonaceous aerosols (CC), carbon monoxide (CO) and ozone (O_3) enhancements due to Asian wildfires and DIAL ozone concentration profile (from top to bottom) along DC8 flight 11.

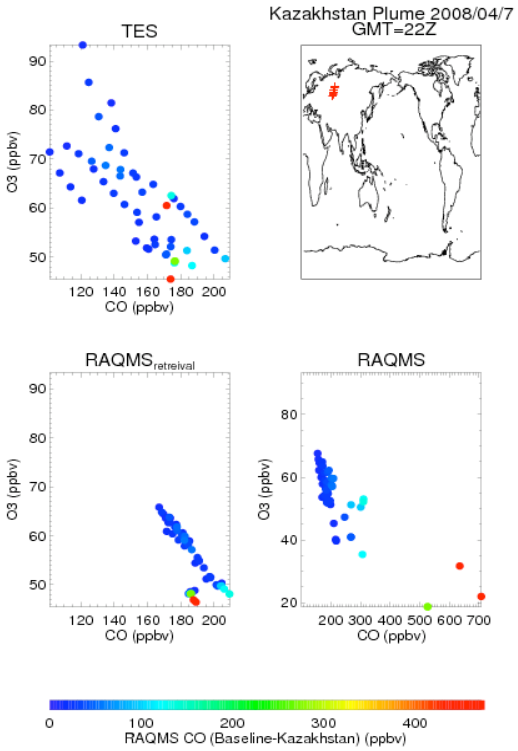

Fig. 11a. Carbon monoxide (CO) and ozone (O_3) concentrations relationship in the plume using RAQMS, adjusted RAQMS and TES results over Kazakhstan fires **(a)**, over Siberian fires **(b)** and around flightlocation **(c)**.

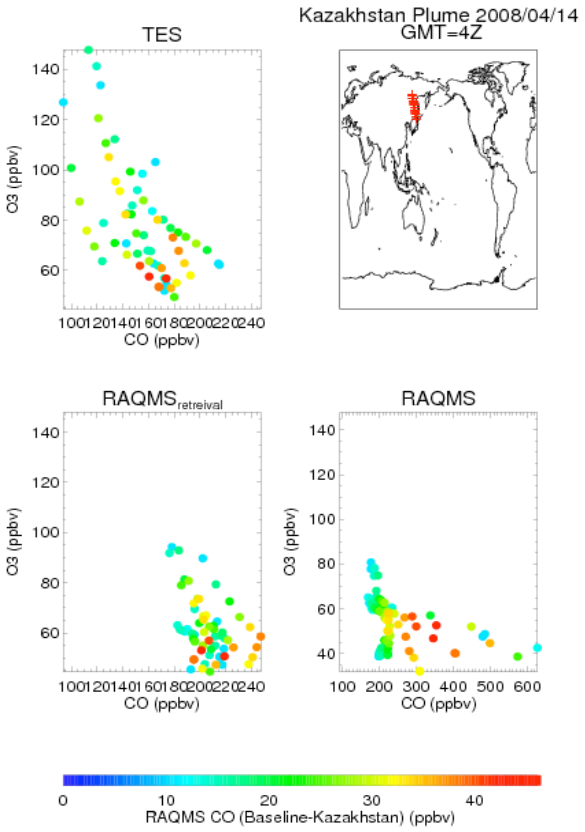

Fig. 11b. Continued.

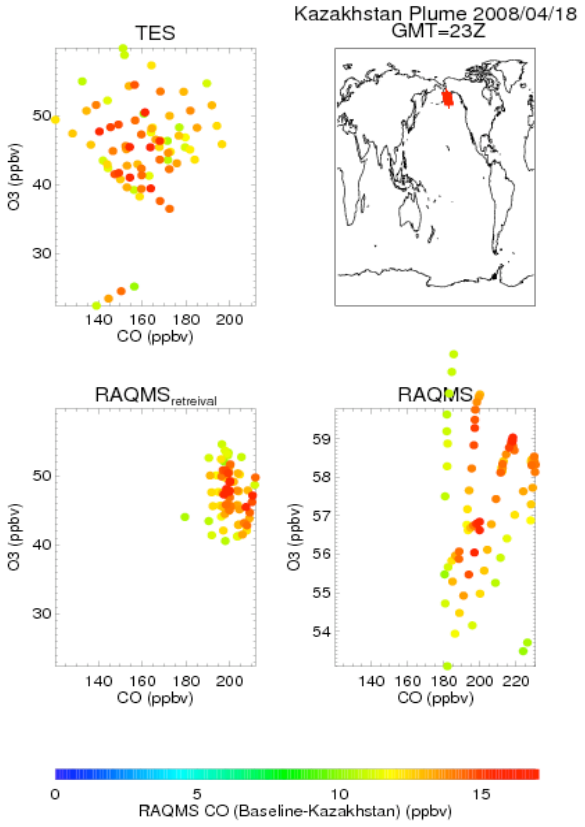

Fig. 11c. Continued.

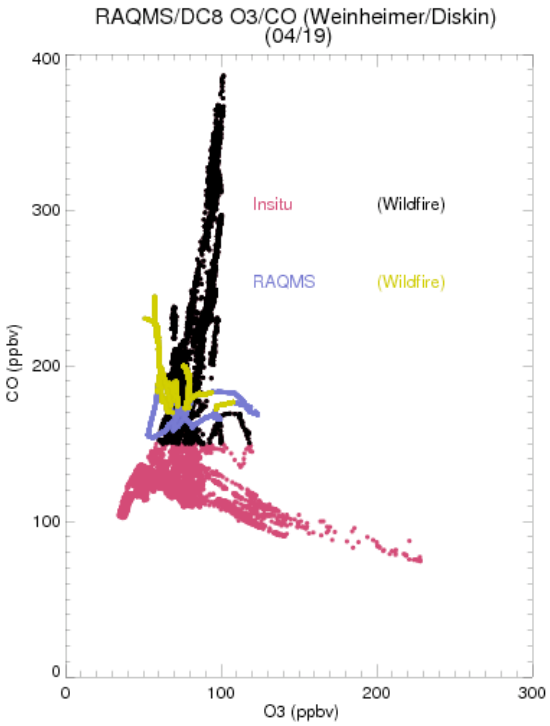

Fig. 12. Carbon monoxide (CO) (ordinate) and ozone (O_3) (abscissa) comparison of background air in situ (pink dots) and RAQMS (blue dots), and wildfire influenced in situ (black dots) and RAQMS (yellow) measurement between around 55° N along DC8 flight 11.

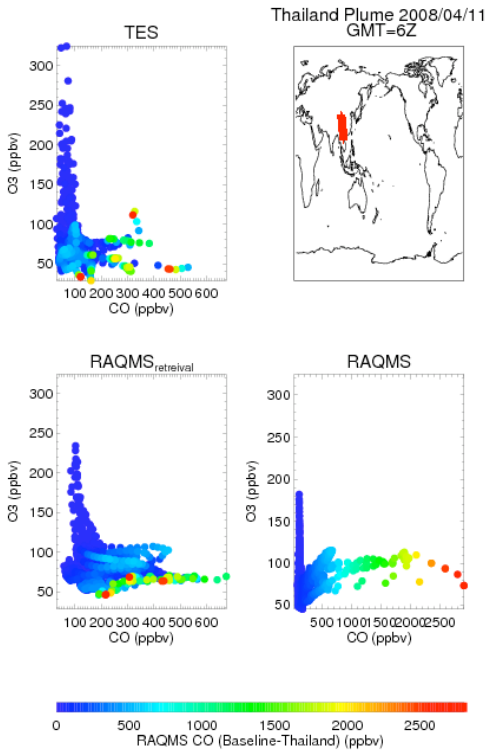

Fig. 13a. Carbon monoxide (CO) and ozone (O_3) concentrations relationship in the plume using RAQMS, adjusted RAQMS and TES results downwind of Thailand fires **(a)**, over the Pacific **(b)** and at flight location **(c)**.

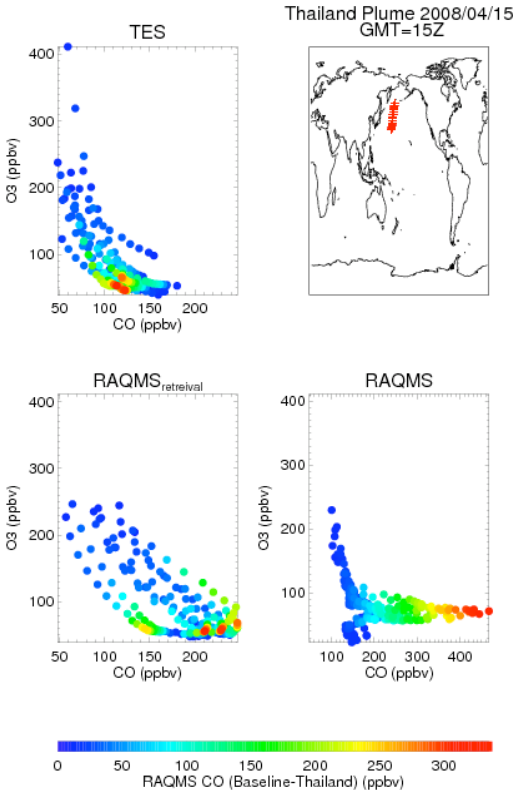

Fig. 13b. Continued.

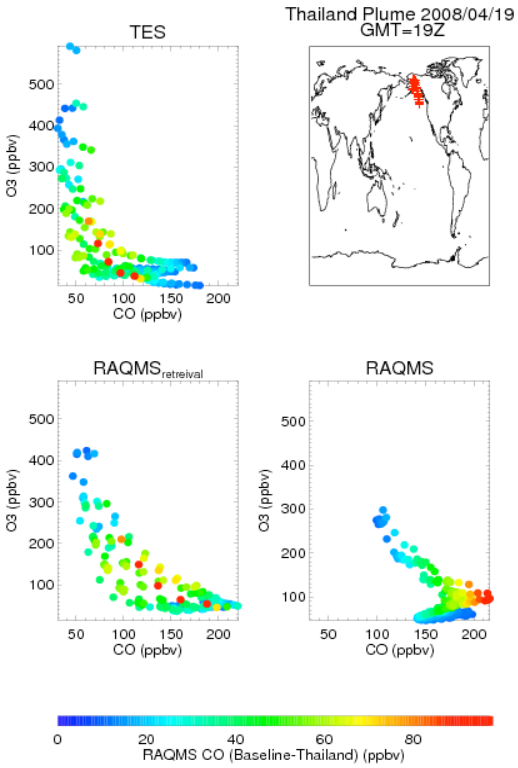

Fig. 13c. Continued.

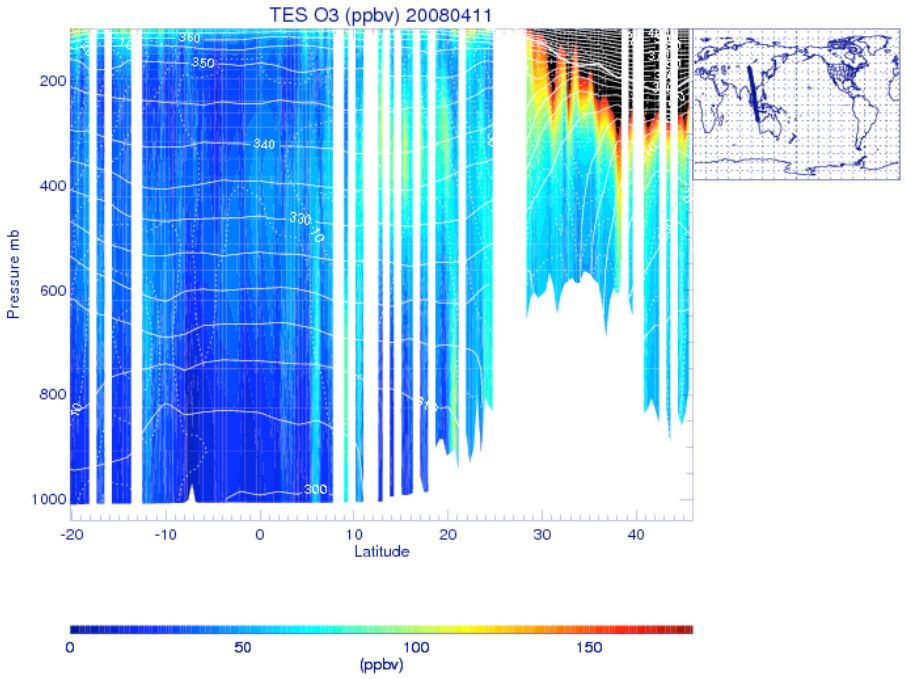

Fig. 14. Ozone (O_3) (left panels) and carbon monoxide (CO) (right panels) profiles from TES, adjusted RAQMS model and adjusted RAQMS model perturbation downwind of Thailand fires during uplifting of the plume via the Tibetan plateau.

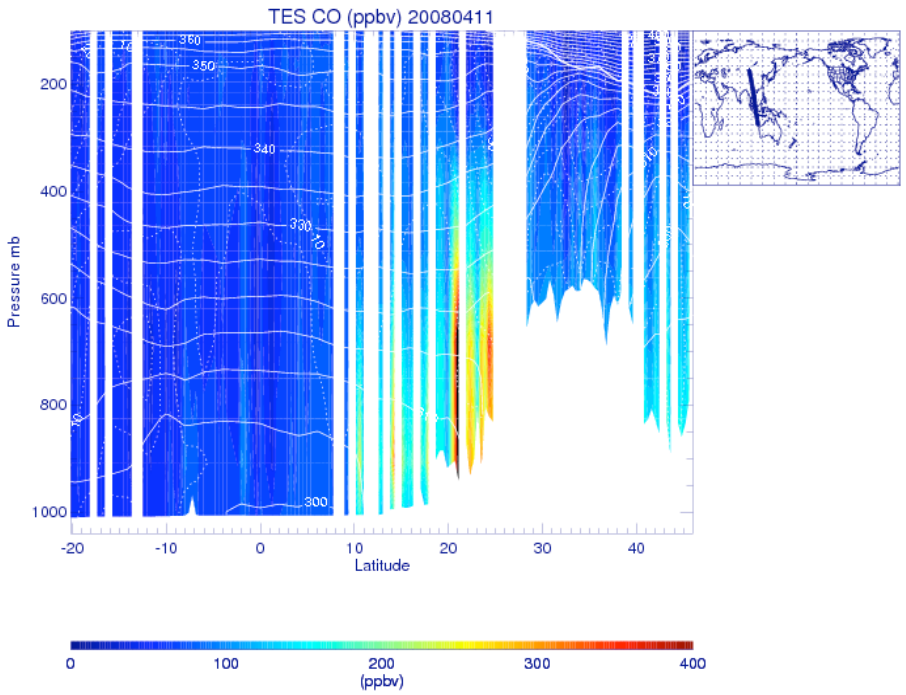

Fig. 14. Continued.

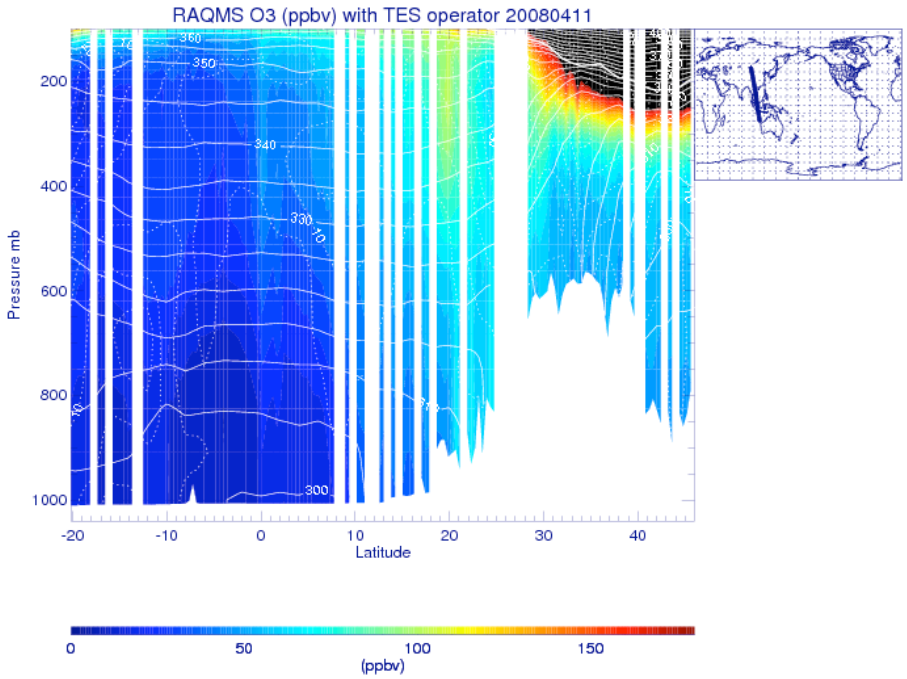

Fig. 14. Continued.

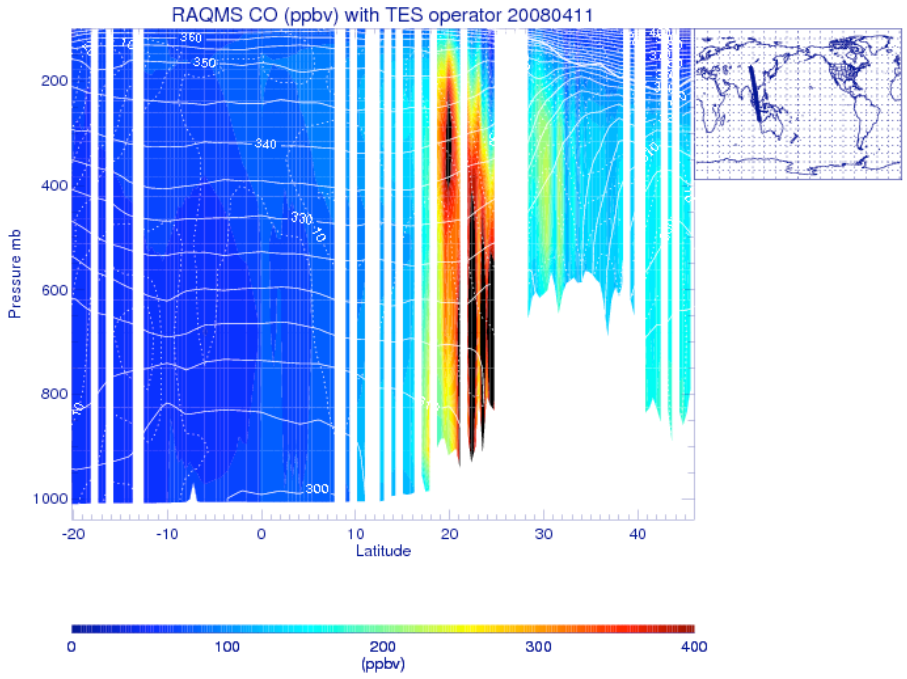

Fig. 14. Continued.

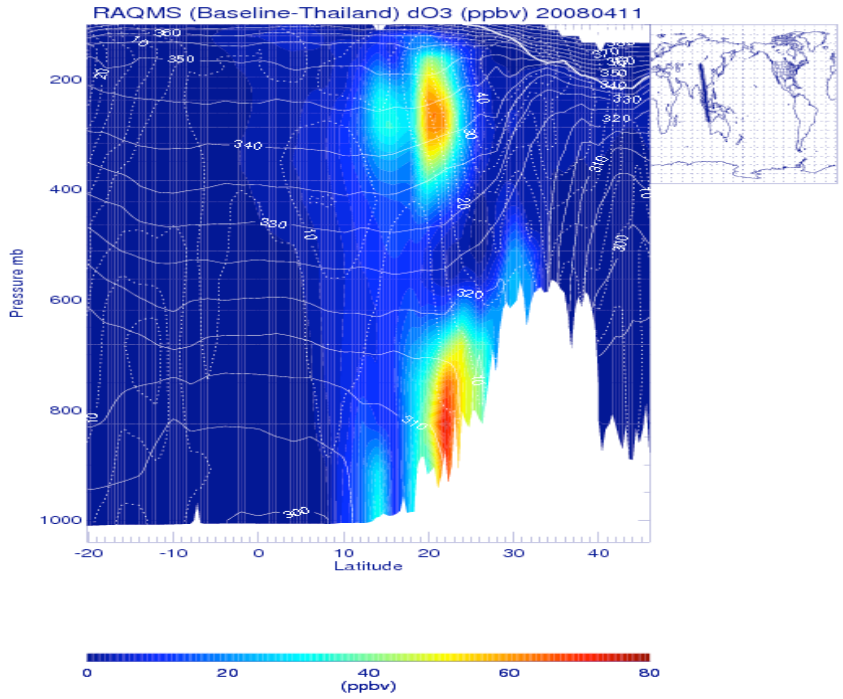

Fig. 14. Continued.

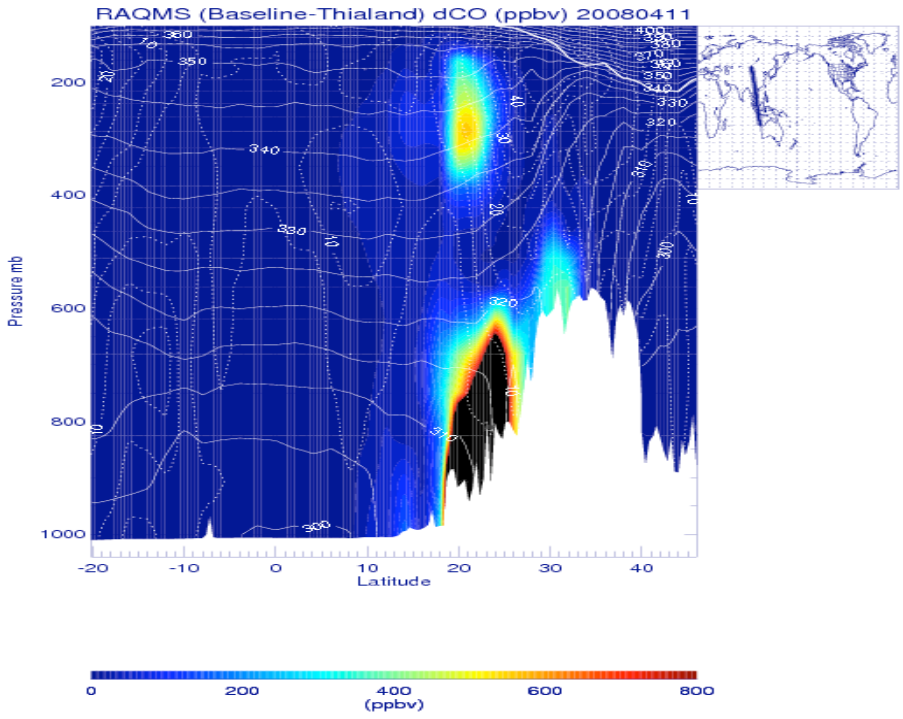

Fig. 14. Continued.

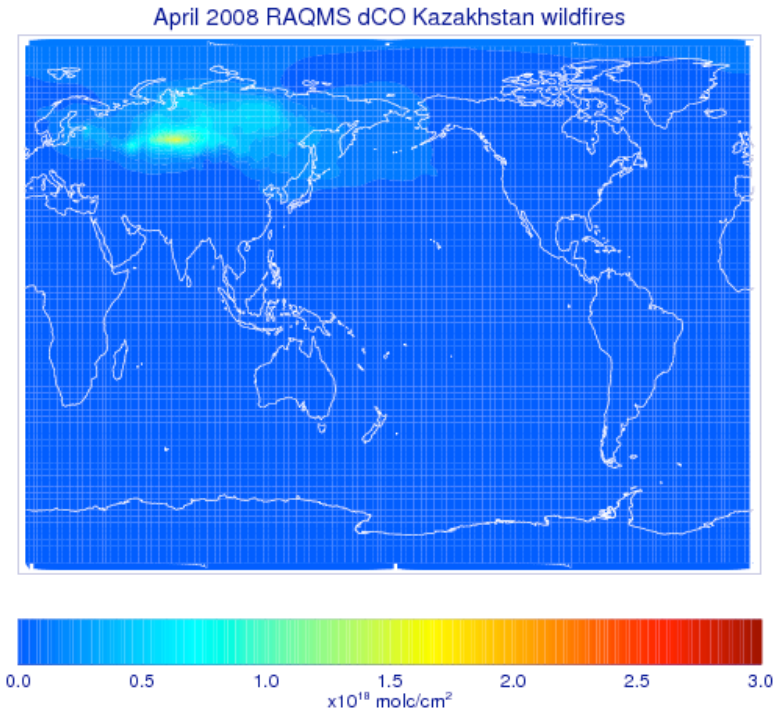

Fig. 15. Monthly dCO and dO_3 from the Kazakhstan fires in April 2008.

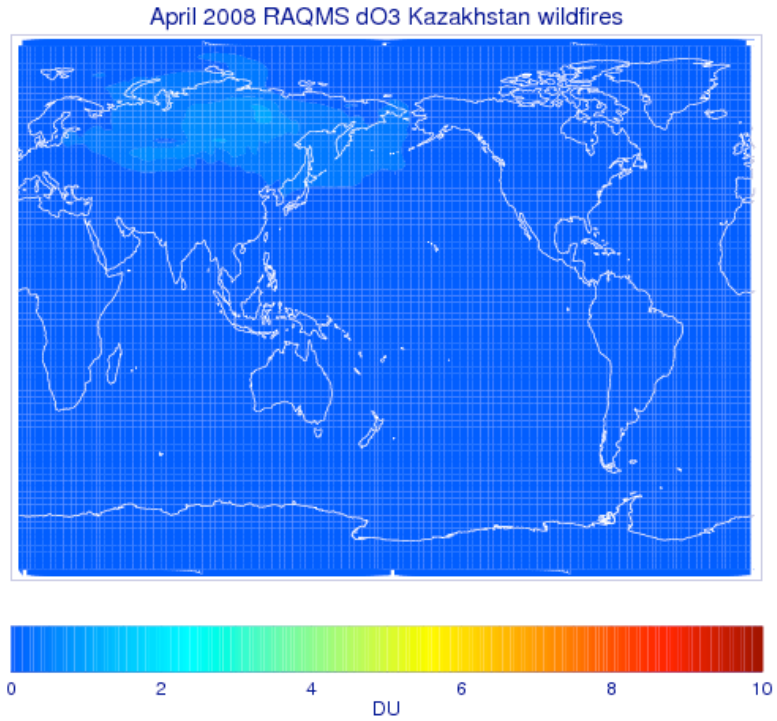

Fig. 15. Continued.

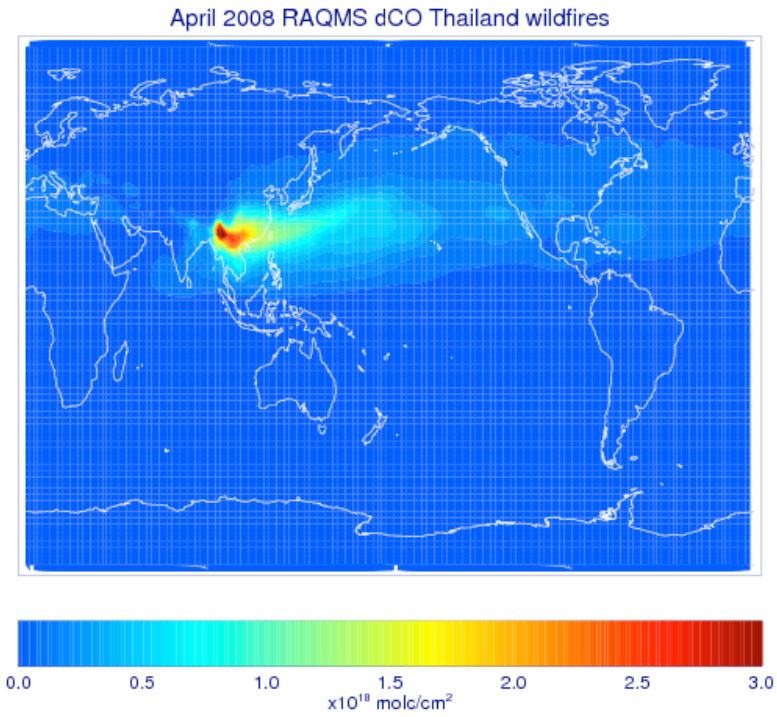

Fig. 16. Monthly dCO and dO_3 from the Thailand fires in April 2008.

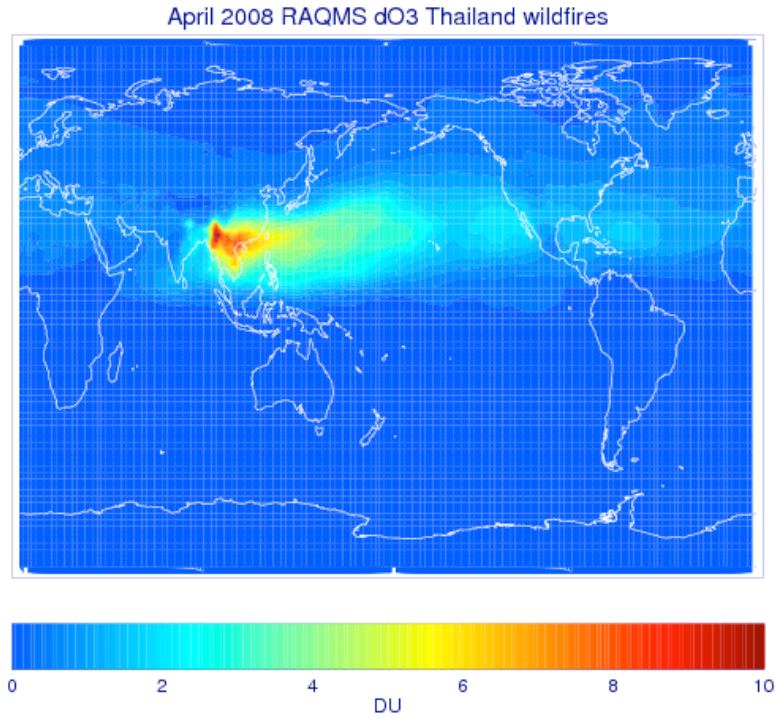

Fig. 16. Continued.